Strategic International Collaborative Research Program (SICORP) Japan-Germany Joint Research Project on Nanoelectronics JST Project End term Report

Japanese Principal Investigator :

<u>Yasuo Ando</u>

(Tohoku University, Professor)

<u>安藤 康夫</u> (東北大学・教授)

Project term: 1/4/2010-31/3/2013

1 The research description during the funding period 公開

研究の概要

背景および研究のねらい

日本ードイツ共同研究「先端スピントロニクス材料と伝導現象(ASPIMATT)」は、これまでのCMOSを置き換えるあるいは凌駕する可能性のある、将来のスピントロニクスのための基盤技術を開発することを目的としている。具体的には、室温におけるデバイス応用のための新しいスピントロニクス材料の開発と新しいスピン伝導(特に面内方向のスピン流)現象に関する研究に焦点を絞る。研究領域としてはナノエレクトロニクスの分野、詳細に言えば、ナノスピントロニクスとそれに関連する材料および構造の研究分野に相当する。

スピントロニクスの分野においては、市場からの強い需要があるにもかかわらず、いまだに多くの問題が解決されずに残っている。ハーフメタルホイスラー合金は、この問題に対して新しい展望を拓くものである。ホイスラー合金は高スピン分極率、高キュリー温度を持つように設計することができる。また、応用によっては、高いスピン注入効率、非常に小さい、あるいは、高いダンピング定数、磁気モーメントの自由な設計(低い磁気モーメントも高い磁気モーメントも実現可能)、異方性の制御なども可能である。このようにしてホイスラー合金は高いポテンシャルを有しているために、これまでの主流である3d-遷移金属系における諸問題を解決できる可能性を秘めている。しかしながら、その化学的(原子の拡散、乱れ)および電子的(ショットキーバリアのデザイン)、スピン特性(スピン注入、スピンポンピング)などにおいて、その界面制御にいまだに問題点を残している。本プロジェクトでは、これらの問題点を解決し、ホイスラー合金を用いた、新しい現象の発見、新しいデバイスの創成を目指している。

このような高い意欲的な目的を達成するためには、必要とされる実験および専門性は一つの場所、あるいは、一つの国のみにおいてできるものではない。このようなことから、本プロジェクトでは二つのドイツの大学、the Johannes Gutenberg Universität Mainz(マインツ大)と the Technische Universität Kaiserslautern(カイザースラウテルン工科大)が、日本からは東北大学が参加し、それぞれの専門性を有機的に結合させている。また、平成25年度からは、ホイスラー合金を用いたデバイス作製に実績を有する、北海道大学も参加する計画である。この組織は、ホイスラー合金のコンピュータベースの物質設計からデバイス作製に至るまでの理解と作製に関して、世界的にみても最高峰の組織であると我々は確信している。

着眼点およびコンセプト

電子は電荷とスピンという二つの自由度を有しているにもかかわらず、これまでのエレクトロニクスにおいては、その電荷のみを用いている。近年、この電子のもつスピンの自由度を用いて、スピン伝導現象をベースとしたデバイス開発を行う研究が行われてきている。このスピントロニクスは不揮発性、低消費電力、スケーラビリティが成り立つという点が特徴であることから、スピントロニクスは将来のナノエレクトロニクスの応用において、技術的に実現可能なもっとも有望な候補である。たとえば一つのチップ上にメモリ機能と演算機能を融合させて、高速かつ再構成可能なメモリを実現するなど、スピントロニクスにより、これまでにない低消費電力デバイスを創成できる可能性を秘めている。

本研究組織においては、1次元および2次元構造におけるスピン伝導、スピン注入、スピン操作、スピン流の検出のための高スピン分極材料および新規材料について研究を行う。共通したスレッドとしては高度な測定技術の応用があげられる。理論面では、界面近傍における磁気的相関に関する基本的現象を取り扱う。また、実験におけるスピンダイナミクスおよび素子の最適化をサポートするために、素子界面における磁気伝導に関する基本的な理解とスピン伝導のための数値モデルの開発を行う。

東北大学(仙台)の研究者は、強磁性トンネル接合および新しい面内スピン伝導素子の作製において世界をリードする技術を有している。カイザースラウテルンのグループは新規の光電子分光およびスピンダイナミクスに関して卓越した技術を有している。マインツ、ドレスデンのグループは、ホイスラー合金のような複雑な金属化合物による新規のスピントロニクス材料の設計と創成および解析に関して先導的な研究を行ってきている。したがって、この研究組織を構成することによって、材料創成、スピン伝導、新規分析技術のような相補的な専門性を集結させることができる。ASPIMATTにおける研究者と、これにより行う個々の研究プロジェクトは、専門性、学術的卓越性、研究方法の相補性の観点から充分に考慮されて構成されている。また、各々のプロジェクトは新規的かつ技術革新の可能性を秘め、両国拠点間の直接の共同研究による付加価値の創成を促すことが期待できる。

ASPIMATT は共通の目的の達成に向けて、二つのプロジェクト領域 (Project Area) および四つの課題 (Task) に分類されている。領域と課題は各々のプロジェクトに対して組織化されている。プロジェクト領域 A は「スピントロニクス応用のための新材料と新機能」である。このプロジェクト領域の主目的は、計算による新材料設計、新材料の創成、および新規分析技術の開発であり、研究対象はバルク材料からヘテロ構造薄膜までを網羅する。ここで新材料は高スピ

ン分極、スピントルク磁化反転における低反転電流、面内スピン伝導のための低スピン散乱レート、マグノン伝導のための低磁気緩和定数、の実現を目指す。実験と理論計算による物性予測はお互いに結果をフィードバックすることにより研究開発を推進させる。プロジェクト領域 B は「スピントロニクスにおける新規の伝導現象」である。このプロジェクト領域では新材料によりもたらされる新規の伝導現象を実現することを主目的とし、新材料を用いたトンネル磁気抵抗(TMR)素子および巨大磁気抵抗(GMR)素子に加えて、ローカル/ノンローカル面内スピン伝導、スピンホール効果およびマグノンによる角運動量伝導のような新しいタイプのスピントロニクスデバイスの創成を目指す。

ASPIMATT は二回の助成期間(3 年+2 年)で計画されている。前半 3 年の四つの課題は、「スピンフィルター効果と垂直方向伝導のための新材料」、「高垂直磁気異方性を有するホイスラー合金」、「ギルバートダンピング(磁気緩和定数)」、「面内スピン伝導とスピン波デバイス」である。これらの課題は、お互いの研究の連携を保つようなコンセプトのもとに設定されている。計算による物質創成のアイディアのもとに新材料の開発を進め、バルクおよび薄膜を作製する。これと並行して、スピン伝導デバイスに開発した新材料を適用する。また、材料の特性の正確な制御およびデバイス界面の改良のために新規の分析技術(光電子分光、X線分光)を、新材料の磁気特性およびスピン伝導現象の研究のためにブリリュアン散乱分光(BLS)を行う。さらに、角運動量伝導に基づく新規の超高速デバイスの開発のために新材料の高周波特性を調べる。後半 2 年については、「ギルバートダンピング」の課題を発展させ、「スピン注入およびダイナミクス」に変更した。ギルバートダンピングの基礎的研究をベースとして、高スピン偏極注入技術の実現や高周波発振素子の開発を行う計画である。その他の三つの課題については、前半に引き続き行うが、単に前半の継続ではなく、画期的な材料特性の向上や、機能性の付与、全く新しい物理現象の発見、デバイスの提案を目指している。

ASPIMATT は 1 年に一回、メンバー全員が集まって会議を開催し、場所は日本とドイツで年ごとに交互に行っている。キックオフミーティングを震災後の 2010 年 10 月に仙台にて行った後、2011 年ドイツ、2012 年仙台と開催した。2013 年はドイツのドレスデンにて会議を行う計画をしている。また、個々のテーマ間では、ビデオコンファレンス等を利用して、二国間の緊密な連携のもとで研究を進めている。また、特殊な測定に関しては、すでに国際共同研究を学生レベルで行っている。また、大学院生の教育のためにジョイントサマースクールも行っており、最先端の研究者を世界中から講師として招聘し。学生の育成にも力を注いでいる。さらに、共同研究を行っている、大学院生は 2 ヶ月程度、他国を含めたパートナー研究室で過ごし、国際経験を積み上げている。

将来展望

ASPIMATT は二回の助成期間(3年+2年)で計画されている。最初の助成期間の中心的課題は、3つあるいは4つの元素からなる新規ホイスラー合金材料の開発である。その材料設計、作製、およびその機能性の評価がプロジェクト領域 A の主な目的である。プロジェクト領域 B は比較的少ないプロジェクト数であるが、新材料を用いた新しい伝導現象について研究を行う。後半の助成期間では、二つのプロジェクト領域の割合を逆にして、むしろ新しく開発した材料をもとにした新規の伝導現象に関するプロジェクトを主に推進させる。特に、材料合成と伝導現象におけるノウハウを基盤にした、面内スピン伝導素子の新しい機能の理解に重点をおく。具体的には、前半に見出された高スピン分極、低ダンピング材料の高性能化に加えて、大きなスピン軌道相互作用を示す新しい材料の開発に取り組む。また、前半では磁気ダンピングが大きな研究の柱の一つであったが、前半で得られた材料、技術をベースとして、後半は低ダンピング材料を用いた高効率スピン注入の実現や、高出力磁性発振素子の開発を行う。以上の理由から、「ギルバートダンピング の課題名を、より大きな目的に相応しい「スピン注入およびダイナミクス」に変更した。さらに、面内デバイスについては、スピン波伝搬素子などの新しいスピンデバイス開発を行うとともに、スピン軌道相互作用を用いた新しいスピン流の生成現象に関する研究を行う計画である。研究期間終了後には、本プロジェクトから、多くの新しい物理現象の発見や、新しいデバイスの提案が期待できる。

本プログラムのグループリーダーのうち何人かは、プロジェクト提案時には、研究経歴の初期段階ともいえる、シニアポスドク(Balke, Chadov, Cinchetti, Serga)(ドイツ)あるいは助教(大兼、永沼、水上、桜庭、好田)(日本)により構成されていたが、ASPIMATTプロジェクトを通じ、多くの実績をあげることで、それぞれキャリアアップを果たしている。また、後半2年のプロジェクトでは、さらに若手の研究者(Liu, Zhan, Ma, 三浦, 栂, Kwilu, Meng, 内田)が加入しており、彼らが海外において研究生活を送ることで、実績を積むとともに、海外の研究者とのネットワークが広がることが期待できる。また、ASPIMATTは若手研究者(博士課程学生、ポスドク)を育成することにも力をいれている。ASPIMATTに所属するそれぞれの若手研究者はお互いの国の研究室を訪問し、あるいは2ヶ月にわたる滞在機会を与えられる。さらに、これらの若手研究者がそれぞれの研究テーマを発表するための特別なワークショップ開催が企画されている。このために、若手研究者の中から代表者を選出して、ASPIMATT運営委員として参加させることを予定している。これらのことから、本プロジェクトを通じて国際舞台で活躍する有望な若手研究者が数多く輩出されることが期待できる。

2 The work done during the funding period 公開

The aim of the Japanese-German Research Unit "Advanced spintronic materials and transport phenomena (ASPIMATT)" was and continous to further develop the foundations for a future spintronics. Key is to use the spin degree of freedom as carrier of information. In the recent years, spintronics has become a wide research field addressed worldwide. First outcomes, such as magnetic sensors based on the giant magnetoresistance and the tunneling magnetoresistance effect have revolutionized the hard-disc industries; novel developments such as spin-transfertorque random access memory are currently aiming at the market.

Key to this field is the development of largely improved magnetic materials and their tailoring to spintronic applications, and this is the central focus of the ASPIMATT research unit. The groups collaborating in ASPIMATT have recognized the need for new materials, and they have opened the new field of the material class of Heusler compounds for spintronic applications. Major contributions to spintronics from the ASPIMATT team have been the development of tetragonal Heusler compounds for spin-transfer torque applications, nowadays used by many other groups as well as industry, high-quality devices for current-perpendicular-plane (CPP) GMR applications with record magneto-resistive parameters, especially for the next-generation read heads in harddisk industries, and, recently, innovative lateral spin transport devices. In the first funding period we have developed and characterized new spintronic materials for applications at room temperature and the fabrication of prototype devices. Now, in the second funding period, as foreseen in the long-term goals, we change the focus more in direction of the study of new devices for spin transport phenomena, in particular lateral spin current phenomena and phenomena related to spin orbit coupling. A novel development in the field is the consideration of effects depending on thermal gradients – spin-caloric effects – and this is now taken up by a specific new project.

In the last funding period large progress has been made to substitute conventional materials by Heusler compounds. The close collaboration between material scientists designing, realizing and characterizing novel bulk and thin-film Heusler compounds and engineers designing new devices has proven extremely fruitful. Groups from two German universities, the Johannes Gutenberg Universität Mainz and the Technische Universität Kaiserslautern, have combined their expertise with groups at the Tohoku University, Sendai, Japan to cover the full range from the computer based design to applications in real devices based on Heusler compounds. In the next funding period, Prof. Felser, who is project leader of German side, will hold two posts of Mainz and MPI, and some members of Mainz have moved in MPI. In addition, two new groups have been added on the Japanese side. Prof. E. Saitoh, a young professor at Tohoku University, brings in his expertise in spin pumping and spin-Seebeck phenomena and will apply them to Heusler compounds. Prof. M. Yamamoto, Hokkaido University, Sapporro contributes with his expertise in epitaxial systems and defect structures. German teams (Kaiserslautern, Mainz, MPI) and Japanese teams (Tohoku, Hokkaido) will continue close collaboration in the next period.

The ASPIMATT team has led to several important breakthroughs in spintronics – in the original proposal we have formulated expected key results.

- 1. Design and synthesis of a Heusler ferromagnetic semiconductor (bulk material and thin films)
 - With Mn₂CoAl the first ferromagnetic Heusler-semiconductors were designed and synthesized as a bulk material [1].
- 2. Design and synthesis of materials for an all-Heusler CPP GMR device, with a metallic/ non magnetic Heusler spacer with a high conductance and an appropriate band structure.
 - An all Heusler device with a magnetic Heusler compounds such as Co₂MnSi and corresponding nonmagnetic semiconductor CoMnTiSi fullfill the desired conductions [2].
- 3. Fabrication of a spin torque device with a Heusler electrode and an RA < 10 $\mu\Omega$ m².
 - The Takanashi group prepared CPP-GMR devices with Heusler electrode, which has low RA [3].
- 4. Demonstration of a lateral spin torque based device

- High-power spin-transfer torque oscillators [4]
- Also the Ando group prepared a lateral device for spin propagation by spin torque oscillation
- 5. 500% TMR at room temperature in a Heusler device
 - 350% TMR achieved at room temperature, and 2000% at low temperature [5].
- 6. 50% CPP GMR at room temperature in a Heusler device
 - Large Magnetoresistance Effect in Epitaxial Co₂Fe_{0.4}Mn_{0.6}Si/Ag/Co₂Fe_{0.4}Mn_{0.6}Si devices [6].
- 7. Understanding dynamics in Heusler devices with low damping
 - Identification of Co₂Mn_{0.6}Fe_{0.4}Si (CMFS) as novel low-damping material with low threshold for applications in nonlinear magnon transport [7].
 - Band-structure dependent ultrafast demagnetization in the Heusler alloy Co₂Mn_{1-x}Fe_xSi [8].
- 8. Demonstration of lateral spin transport in Heusler devices
 - Realization of lateral spin-valve devices with half-metallic Heusler compounds in the Takanashi group (Project 4.6-B).

The record value in CPP-GMR devices being achieved with Heusler compound electrodes by the ASPIMATT team attracted already the interest of the hard disc industry. Within the first funding period the ASPIMATT principle investigator have jointly contributed to nearly all areas of spintronics research and proven the high impact of Heusler compounds due to their tunability. All the requirements for STT-RAM, low damping with low magnetization and high spin polarization are impossible to find in traditional magnetic materials, but in the new class of manganese rich Heusler compounds.

After our discovery of the unique properties of bulk Mn₃Ga and thin films [9,10] many companies (IBM with Micron, Intel and Seagate) have started to investigation of Mn₃Ga and related systems for STT-RAM and STT Oscillators. Additionally the Mizukami and Miyazaki group could show that high frequency oscillation can be realized. Spin precession with frequencies up to 280 GHz is observed in Mn_{3-x}Ga alloy films with a perpendicular magnetic anisotropy constant K_u of 15 M erg/cm³. The damping constant α, characterizing macroscopic spin relaxation and being a key factor in spin-transfer-torque systems, is not larger than 0.008. Those are about one-tenth of α-values for known materials with large K_u [11]. However, one drawback is a low TMR value, to low by a factor 3. In a strong collaboration between the German and Japanese group we were able to identify several potential reasons and solutions.

A smooth interface is critical for a high spin polarization, but can be designed with the help of a dusting layer (Co, Fe). The lattice mismatch can be overcome by searching for a Mn2YSn compound with a high Curie temperature and band structure match to MgO. Another way was established in collaboration between Mizukami/Myazaki and Felser/Fecher groups by increasing the number of valence electrons when using Mn3-xCoxGa [12] instead of Mn3-xGa. The recently produced and investigated thin films exhibit perpendicular anisotropy with high coercive fields [13]. They are right now in the optimization stage and will be used in the next funding period for devices. The Yamamoto team discovered the highest TMR ratio in a Heusler compound with Heusler electrodes containing access manganese [5]. This is not surprising because both families, Co2- and Mn2-based Heusler compounds, are 100% spin polarized in the bulk. For the second funding period Yamamoto has joint ASPIMATT, he had already a joint JST-DFG project with the Felser group from 2009-2011. Within this collaboration, the world wide first spin resolved high energy photoelectron spectroscopy experiments were performed in Japan and Germany [14].

With spincalorics a new field was introduced to spintronics, which has caused the attraction of nearly all groups working in spintronics worlds wide. Saitoh and his team is therefore the second new group of the ASPIMATT team and his series of recent high impact publications speak for themself. In the area of lateral spin transport the CPP-GMR with continuous Co₇₅Fe₂₅ free layer prepared on a coplanar wave guide with low microwave transmission loss for BLS measurement was a further high light of the first funding periode. The Spin Torque Oscillation was observed electrically without harmonic signal (Ando and Hillebrands).

The partners of ASPIMATT published overall more than 100 papers in refereed journals. From those 10 are coauthored jointly by Japanese and German teams, 52 by Japanese teams, and 39 by

German teams. Further, seven PhD theses were successfully finished in the German groups of ASPIMATT. The members of ASPIMATT gave 106 invited and 134 contributed talks on national and international conferences.

Notwithstanding natural disasters (flight cancellation due to volcano eruption and earthquake), the ASPIMATT consortium was able to held two joint meetings together with one summerschool and to keep researchers exchange between Japan and Germany active.

References

- [1] S. Ouardi, G. H. Fecher, J. Kübler, and C. Felser, "Realization of spin gapless semiconductors: the Heusler compound Mn₂CoAl", Phys. Rev. Lett. 110, 110401 (2013).
- [2] S. Chadov, T. Graf, K. Chadova, X. Dai, F. Casper, G. H. Fecher, and C. Felser, "Efficient Spin Injector Scheme Based on Heusler Materials," Phys. Rev. Lett. **107**, 047202 (2011).
- [3] Y. Sakuraba, K. Izumi, T. Iwase, S. Bosu, K. Saito, K. Takanashi, Y. Miura, K. Futatsukawa, K. Abe, and M. Shirai, "Mechanism of large magnetoresistance in Co₂MnSi/Ag/Co₂MnSi devices with current perpendicular to the plane", Phys. Rev. B **82** (9), 094444 (2010).
- [4] R. Okura, Y. Sakuraba, T. Seki, K. Izumi, M. Mizuguchi, and K. Takanashi, "High-power rf oscillation induced in half-metallic Co₂MnSi layer by spin-transfer torque", Appl. Phys. Lett. **99**, 052510 (2011).
- [5] H. Liu, Y. Honda, T. Taira, K.-i. Matsuda, M. Arita, T. Uemura, and M. Yamamoto; "Giant tunneling magnetoresistance in epitaxial Co₂MnSi/MgO/Co₂MnSi magnetic tunnel junctions by half-metallicity of Co₂MnSi and coherent tunneling", Appl. Phys. Lett. **101**, 132418 (2012).
- [6] J. Sato, M. Oogane, H. Naganuma, and Y. Ando; "Large Magnetoresistance Effect in Epitaxial Co₂Fe_{0.4}Mn_{0.6}Si/Ag/Co₂Fe_{0.4}Mn_{0.6}Si Devices", Appl. Phys. Expr. **4**, 113005 (2011).
- [7] T. Sebastian, Y. Ohdaira, T. Kubota, P. Pirro, T. Brächler, K. Vogt, A. A. Serga, Hiroshi Naganuma, M. Oogane, Y. Ando, and B. Hillebrands, "Low-damping spin-wave propagation in a micro-structured Co₂Mn_{0.6}Fe_{0.4}Si Heusler waveguide", Appl. Phys. Lett. **100**, 112402 (2012).
- [8] D. Steil, S. Alebrand, T. Roth, M. Krauß, T. Kubota, M. Oogane, Y. Ando, H. C. Schneider, M. Aeschlimann, and M. Cinchetti, "Band-Structure-Dependent Demagnetization in the Heusler Alloy Co₂Mn_{1-x}Fe_xSi", Phys. Rev. Lett. **105** (21), 217202 (2010).
- [9] B. Balke, G. H. Fecher, J. Winterlik, and C. Felser, "Mn₃Ga, a compensated ferrimagnet with high Curie temperature and low magnetic moment for spin torque transfer applications", Appl. Phys. Lett. **90**, 152504 (2007).
- [10] F. Wu, S. Mizukami, D. Watanabe, H. Naganuma, M. Oogane, Y. Ando, and T. Miyazaki, "Epitaxial Mn_{2.5}Ga thin films with giant perpendicular magnetic anisotropy for spintronic devices", Appl. Phys. Lett. 94, 122503 (2009).
- [11] S. Mizukami, F. Wu, A. Sakuma, J. Walowski, D. Watanabe, T. Kubota, X. Zhang, H. Naganuma, M. Oogane, Y. Ando, and T. Miyazaki, "Long-Lived Ultrafast Spin Precession in Manganese Alloys Films with a Large Perpendicular Magnetic Anisotropy", Phys. Rev. Lett. 106, 117201 (2011).
- [12] V. Alijani, J. Winterlik, G. H. Fecher, and C. Felser, "Tuning the magnetism of the Heusler alloys Mn3-xCoxGa from soft and half-metallic to hard-magnetic for spin-transfer torque applications", Appl. Phys. Lett. **99**, 222510 (2011)
- [13] S. Ouardi, T. Kubota, G. H. Fecher, R. Stinshoff, S. Mizukami, T. Miyazaki, E. Ikenaga, and C. Felser, "Stoichiometry dependent phase transition in Mn-Co-Ga-based thin filmsFrom cubic in-plane, soft magnetized to tetragonal perpendicular, hard magnetized", Appl. Phys. Lett. 100, 242406 (2012).
- [14] A. Gloskovskii, G. Stryganyuk, G. H. Fecher, C. Felser, S. Thiess, H. Schulz-Ritter, W. Drube, G. Berner, M. Sing, R. Claessen, M. Yamamoto; "Magnetometry of buried layers-Linear magnetic dichroism and spin detection in angular resolved hard X-ray photoelectron spectroscopy", J. Electron Spectrosc. Relat. Phenom. 185 (2012) 47.

2.1 Objectives

Building on the framework of the first funding period, we continue to follow the two main objectives:

- 1. Development of new Heusler materials with advanced properties for spintronic applications,
- 2. Exploration of new transport phenomena in spin electronics based on Heusler materials, with increased focus on the second objective.

ASPIMATT continues to be organized by two Project Areas, reflecting these two objectives, and, as a separate sorting category, into four Tasks addressing specific common goals. The Project Areas and the Tasks provide a matrix for the projects. Table 1 shows the matrix with the projects. All ASPIMATT partners and their projects have been carefully selected with respect to expertise, scientific standing, complementarity in research methods as well as with respect to novelty, potential for innovation and generating added value via collaboration, in particular via direct cooperation between groups from both countries. In the new funding period, emphasis is shifted towards applications, as foreseen in the long-term vision in the original proposal. Therefore, some projects (2.2-A, 2.3-A, 3.1-A, 4.3-B) have been brought to an end – all these projects have achieved their anticipated goals. Two new groups have been added on the Japanese side. Prof. E. Saitoh, a young professor at Tohoku University, brings in his expertise in spin pumping and spin-Seebeck phenomena and will apply them to Heusler compounds. Prof. M. Yamamoto, Hokkaido University, Sapporro contributes with his expertise in epitaxial systems and defect structures. Other projects have been adjusted to address the new directions.

The project areas are

Project Area A: New materials with advanced properties for spintronic applications

Project Area B: New transport phenomena in spin electronics

And the tasks are continued as well:

Task 1: New materials for spin filter effect

Task 2: Heusler alloys with large perpendicular anisotropy

Task 3: Spin injection and dynamics

Task 4: Lateral spin transport and spin waves including devices

Building on the results obtained in the first funding period, we formulate the following expected key results for the second funding period:

- 100% room temperature TMR for tetragonal Heusler compounds for spin-transfer torque application
- Novel Heusler based spin injector materials for Si with MR ratio beyond state of the art
- Demonstration of magnetic switching by a pure spin current in a lateral Heusler based device
- CPP Heusler based spin-torque oscillators with large output power and high q-factor
- Development of materials with improved low Gilbert damping
- Development of a Heusler material for giant spin-Hall effect to replace Pt in all-Heusler spin pumping, spin-Hall effect devices and realization and characterization of such devices
- Understanding spin-pumping and spin-Seebeck mechanisms in Heusler based heterostructures
- Spin-wave propagation, nonlinear dynamics and phase locking in Heusler materials
- Direct measurement of spin-injection efficiency and understanding of the dynamics on the femtosecond time scale

From the viewpoint of applications spintronics and therefore ASPIMATT has become even more relevant during the past three years. Over the last decade, there are more and more demanding users of an entirely new range of electronic devices designed to facilitate communication, exchange ideas and strengthen social bonds. The common denominator of these devices is their dependency on cheap, fast and reliable non-volatile mass storage, retained in the absence of power. During the

first quarter of 2010, a total of 3,397 petabytes (1015 B) of storage capacity was shipped from the suppliers to their customers (source: Inter-national Data Corporation). Intel alone predicts that their corporate storage needs will balloon from 20 PB in 2007 to 90 PB in 2012 (Intel white paper on storage cost). EMC predicts that the global need for storage will increase 44-fold by 2020, mainly driven by the need for massive on-line storage [15]. This huge projected increase of memory highlights the need to improve memory performance, both in terms of density and power consumption, as the limits of the current technology are already being approached. The future of storage requires development of new materials that combine the strengths of the existing technologies while suppressing their weaknesses.

Whereas the hard-disk drive has been the mass storage technology of choice for over 50 years, solid state memory is also of primary importance both for storage (cf. the rapidly growing use of solid state drives in PCs, tablets and handheld devices) and for cache between processors and memory, on the one hand, and users and data centres, on the other hand. The solid-state memory market is a multi-billion dollar business and expected to increase from \$46.2 Billion in 2009 to \$79 Billion in 20142, with three major technologies currently in play: DRAM (60% of the market volume) as a fast, dense and cheap (albeit volatile) memory, Flash (30%) as the non-volatile (e.g. storage) memory and SRAM (10%), as fast cache memory. Whilst Flash capacity is rapidly increasing towards hard-disc drive (HDD), it remains limited due to higher cost, low writing speed and limited endurance. SRAM and DRAM both suffer from their volatility and there are scalability issues beyond 22 nm feature size.

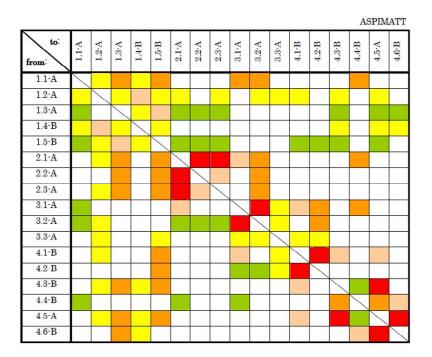
Among the magnetic RAMs the Spin-Transfer-Torque Magnetic RAM (STT-MRAM) is one of the two most promising emerging memory devices for non-volatile data storage (according to the Semiconductor Research Corporation, 2011). Moreover, STT-MRAM has perspectives below the 10 nm feature size, because STT for magnetisation switching (writing) can be supported by localized heating during write, similar to Heat-Assisted Magnetic Recording (HAMR) in hard disk drives. Within this approach, labelled TAS (Thermally-Assisted Switching), new magnetic storage materials with extremely high anisotropy, low magnetisation and low damping can open the way to further increase thermal stability while targeting write times well below 10nsec. In addition, STT combined with TAS then can reduce power consumption per write cycle to a minimum, possibly down to the fJ range at a 10nm feature size.

2.2 Work programme incl. proposed research methods

It is evident, that the aims of ASPIMATT can only be achieved via a very strong and well managed collaboration. The team building process between the ASPIMATT members has been extremely successful. The organization of the ASPIMATT collaboration has worked out very well and will be continued. Projects have been arranged by criteria of quality, optimum complementarities and interaction. For reasons of easy financial management joint German-Japanese projects have not been foreseen. However, only projects have been accepted into ASPIMATT, which have strong direct links and need for collaboration to the other country. These links are described in each project description.

The interaction between the projects is shown in Table 1. Projects with very strong interaction are marked with red, those which are complementary are marked with pink. Projects which provide samples to others are marked in orange, projects which supply theoretical support and predictions in yellow, and projects which provide some service to others in green.

Table1Matrix of interactions between projects. Red: projects with very strong interaction; rose: collaboration and complementary projects; orange: projects which provide samples and ideas to others; yellow: projects which supply theoretical support; green: projects which provide service to others to some extent.



The ASPIMATT initiative will meet once year with all members, alternating between Japan and Germany. Smaller, thematically focused workshop meetings such as on specific materials aspects and on transport problems will be organized, in addition. In the day-to-day business means such as video conference tools, will be used in addition to standard telephone calls and e-mails. Specific measures, which have been proven to work very successfully, will be continued to foster the international collaboration already on the student level. For the training of the graduate students one joint summer school on an innovative subject is planned for 2014 in Japan, succeeding the international summer school organized in Kaiserslautern in 2011. Leading scientists from around the world will be invited as lecturers. These actions will of course be reinforced by other dissemination actions (publications, submissions to international conferences etc). Graduate students are expected to spend secondment of at least two months duration in partner lab in the other country, and student workshops organized by the students themselves are strongly encouraged.

2.3 Important results

1.1-A New materials for controlling high spin polarized current with low electric consumption

(I) Heusler materials

In this section, we will report the tunnel magnetoresitance effect in junctions with Co₂Fe(Al,Si) full-Heusler electrodes to obtain the highly polarized spin current in conjunction with their crystal structure, and spin injection phenomena into GaAs semiconductor from Co₂Fe(Al,Si) full-Heusler electrodes which generate highly spin polarized current.

junctions with stacking ofCr-bufferd MgO single а structure crystal substrate/Co₂FeAl_{0.5}Si_{0.5} 30 nm/Al1.3nmoxide/ Co₇₅Fe₂₅ 3 nm/IrMn15nm/Ta were also fabricated. The Al-oxide barriers were formed by plasma oxidation for 120 s in the chamber. The junctions were patterned by using conventional electronbeam lithography and Ar ion etching. The patterned junctions were annealed at optimized temperature between 200C and 350C in high vacuum by applying a 2 kOe magnetic field. Magnetoresistance curves were measured by a four-probe method from 5 K to RT. The junction on MgO(100) exhibited 76% at RT and 106% at 5 K, while that on MgO(110) showed 72% and 103% at RT and 5 K, respectively. The largest magnetoresistance ratio in this study is derived from the highly ordered B2 structure, not L21 structure. From the results of magnetization and surface roughness measurement, the Co₂FeAl_{0.5}Si_{0.5} with L2₁ structure obtained by 600C annealing, possesses as small magnetization and large surface roughness. These will be the reason of the smaller tunneling spin polarization of L2₁ structure due to the imperfect L2₁ ordered structure or rough interface due to Cr inter diffusion from the buffer layer. By applying the spin polarization of 0.5 for Co₇₅Fe₂₅ into Julliere's model, the tunnel spin polarization, which includes the effect of barrier parameter, interface between barrier and electrode, and ferromagnetic electrode spin polarization, of Co₂FeAl_{0.5}Si_{0.5} fabricated on MgO (100) and MgO (110) is estimated to be respective 0.71 (0.55) and 0.70 (0.53) measured at 5 K (RT), respectively.

The tunnel magnetoresistance effect for junctions with Co₂FeAl_{0.5}Si_{0.5} electrodes and MgO (001) epitaxial barrier was investigated to improve the magnetoresistance ratio. First Co₂FeAl_{0.5}Si_{0.5} electrodes and MgO barrier was fabricated by sputtering and MBE systems, respectively. In this junction, maximum magnetoresistance ratio of 390% (220%) measured at 5 K (RT) was obtained, which correspond to spin polarization of 0.81 (0.72). Next, both Co₂FeAl_{0.5}Si_{0.5} electrodes and MgO barrier were fabricated by MBE system. In this case, Co₂FeAl_{0.5}Si_{0.5} electrodes were fabricated by MBE with two kinds of annealing treatments. That is, annealing treatment is carried out during and after deposition for a lower Co₂FeAl_{0.5}Si_{0.5} electrode. The maximum magnetoresistance ratio of 832% (386%) measured at 9 K (RT) was obtained, which correspond to tunnel spin polarization of 0.90 (0.81). In this study, all layers were fabricated by MBE system in ultra-high vacuum conditions, which might be attributed to the improvement in the MgO barrier quality.

(II) Spin filter

The magnetic moment has been reported to increase when the Fe atom in BiFeO₃ is replaced with Co atom. As a result, these materials are in growing demand for use in spin-filter applications with low electric consumption during the writing process. When used for spin-filter structure, a few-nanometer-thick high-quality film, a flat surface/interface, and good compatibility with the thin metal film process are required. The aim in first funded period is to determine the preparation conditions of single phase Co-substituted BiFeO₃ [Bi(Fe_{0.9}Co_{0.1})O₃] epitaxial films on SrTiO₃ (100) substrates by r.f. magnetron sputtering.

The Co-substituted BiFeO₃ films having a thickness of 50 nm were fabricated by r.f. magnetron sputtering on single crystal SrTiO₃ (100) substrates. The sputtering target of Bi(Fe_{0.9}Co_{0.1})Ox consisted of Bi₂O₃ and Fe₂O₃ powder that had been sintered in air. The sputtering conditions such as argon (Ar) and/or oxygen (O₂) gas pressure, sputtering power, heating temperature in vacuum or air were systematically changed to fabricate single phase Bi(Fe_{0.9}Co_{0.1})O₃ films.

The films deposited by r.f. magnetron sputtering using Ar and Ar + O₂ gases at an ambient temperature had an amorphous structure. In order to crystallize the perovskite structure of

Bi(Fe_{0.9}Co_{0.1})O₃ films, the samples were annealed under both vacuum and air conditions. In the case of the samples annealed under vacuum conditions, secondary phases such as BiO_x were formed; therefore, the experimental data of the vacuum condition is not shown. The formation of the perovskite structure in XRD patterns was identified by the high angle peak of (003) Bi(Fe_{0.9}Co_{0.1})O₃, because the lattice mismatch decreased with increasing Co content. The films crystallized above the annealing temperature of 500°C with a broad unknown peak of $2\theta = 27^{\circ}$, however, the perovskite phase was not observed at 500°C. After annealing at 600°C, only the perovskite peaks of (003) Bi(Fe_{0.9}Co_{0.1})O₃ was observed near the peaks of the (003) SrTiO₃ substrate. At 700°C, the secondary phases of BiO_x were observed, and the peak of the perovskite structure became weak.

The magnetic property of single phase Bi(Fe_{0.9}Co_{0.1})O₃ epitaxial films was measured. A saturation magnetization of 20 emu/cm³ was observed along with a weak remanent magnetization. When compared with epitaxial and polycrystalline BiFeO₃ films, the magnetization was clearly enhanced. This magnetization might be attributed to local ferrimagnetism and/or suppression of long-range incommensurate spin cycloids and/or moderation of short-range canted *G*-type antiferromagnetism. In order to compare our results with previous works, we plotted magnetization values as a function of Co concentration. A magnetization of 20 emu/cm³ at a Co concentration of 10 at.% is almost consistent with previous reports that used a different preparation method.

1.4-B Theoretical studies on electronic and transport properties of heterostructures based on half-metallic Heusler alloys

(I) First-principles study on temperature dependence of tunneling magnetoresistance of magnetic tunnel junctions with Co₂MnSi

In order to elucidate the mechanism of the large temperature dependence of the TMR ratios, we theoretically investigate the effect of thermal fluctuation of the local spin-moment to the TMR effect.

We found that the G_P (G_{AP}) decreases (increases) with increasing spin angle θ , leading to the significant reduction of the TMR ratio (less than 100% at θ =45° for both MTJs). These results can be attributed to the spin-flip scattering of conducting electrons owing to the interfacial noncollinear magnetic structures. Furthermore, we estimated the exchange coupling of interfacial Co spin-moments in the CMS/MgO junction and found that the interfacial exchange constant is much smaller than that of bulk CMS. This results in large temperature dependence of the TMR ratio for the Co-terminated CMS/MgO/CMS MTJ comparing with the Fe/MgO/Fe MTJ, which is consistent with recent experimental results. These results indicate that the low TMR ratio observed in the CMS/MgO/CMS MTJs at RT is attributed to the spin-flip scattering at the interfacial Co-layers of the MTJs caused by the non-collinear magnetic structures as a result of the thermal fluctuation of interfacial Co spin-moments.

(II) First-principles study on ballistic transport properties in Co₂MnSi/X/Co₂MnSi(001) (X=Ag,Au,Al,V,Cr) tyrilayers"

Recently, the current-perpendicular-to-plane (CPP) giant magnetoresistive (GMR) devices on the basis of the half-metallic Co₂YZ have been fabricated. Although the observed magnetoresistive effects in CPP-GMR devices are rather small compared with those in TMR devices, studies on the CPP-GMR system are still important because of the small resistance area product (RA), which is crucial for realization of an ultra-high-speed reading in magnetic read heads of hard disk drives (HDD). We investigate and discuss the origin of interface resistance in magnetic trilayers with the half-metallic Co₂MnSi by performing first-principles electronic structure and ballistic transport calculations for CMS/X/CMS(001) (X=Ag,Au,Al,V,Cr).

It is found that the averaged transmittance of the trilayer with anti-ferromagnetic (AFM) bcc-Cr spacer is about $0.2\sim0.3\,G_0$, which is $1/5\sim1/3$ of smaller than that with other spacer. These results qualitatively agrees with recent experimental results on CPP-GMR devices of epitaxial

CMS/Ag/CMS and CMS/Cr/CMS, where the smaller resistance area product of the CMS/Ag(001) interface than that of the CMS/Cr(001) has been obtained. It is clearly seen in our calculation that the conducting channels of CMS/Cr/CMS are restricted in a small region around k_{\parallel} =(0,0). On the other hand, highly conducting channels spread over almost entire region in the k_{\parallel} plane for CMS/Ag/CMS. The highly conducting region in the k_{\parallel} plane can be understood qualitatively by considering the matching of the Fermi surface over the k_{\parallel} -plane between CMS and Ag comparing with AFM-Cr. These results indicate that the matching of the Fermi surface projected to the 2d-BZ of k_{\parallel} is a main contributing factor for the spacer-dependence of the interfacial resistance.

(III) Magnetoresistance Effect in Tunnel Junctions with Perpendicularly Magnetized $D0_{22}$ -Mn_{3- δ}Ga and MgO Barrier

In this study, we have investigated the TMR effect in MgO-based MTJs with D0₂₂-Mn₃Ga by using the first-principles electronic and ballistic-transport calculations. First, we have calculated the electronic band-structure of bulk $D0_{22}$ -Mn₃Ga. The dispersion curves along the [001] direction are depicted for the majority- and the minority-spin states, respectively. It is found that the totally symmetric Δ_1 band in Mn₃Ga crosses the Fermi level both in the majority- and minority-spin states, in contrast to ferromagnetic transition metals such as bcc Fe. The minority-spin Δ_1 band is predominantly composed of Mn $d(3z^2 - r^2)$ orbital at the Fermi level, while the majority-spin Δ_1 band is mainly constructed from Ga-p(z) orbital.

Then, we have investigated the tunneling conductance of Mn₃Ga/MgO(1nm)/ Mn₃Ga(001) MTJs with the MnMn-termination and MnGa termination. Tunneling transmittance calculated at k_{\parallel} = (0, 0) is depicted as a function of incident electron energy relative to the Fermi level for the Mn-Mn termination in the parallel magnetization configuration via the majority- and the minority-spin channels, respectively. It is confirmed that the Δ_1 band predominantly contributes to the tunneling transmittance for both the majority- and the minority-spin channels. Furthermore, it is noted that the tunneling transmittance via the majority-spin channel is almost two orders of magnitude larger than that via the minority-spin channel at the Fermi level. The significant reduction of the tunneling conductance at the Fermi level of the minority-spin channel can be attributed to the scattering of $d(3z^2 - r^2)$ electrons at Mn₃Ga/MgO(001) interface, since Mn $d(3z^2 - r^2)$ orbital is much more localized than Ga-p(z) orbital. As the consequence, we have obtained the positive TMR ratio 642% for the MTJ with the MnMn termination exceeding and 70% for the MnGa termination.

(IV) First-principles study of tunneling magnetoresistance in Fe/MgAl $_2$ O $_4$ /Fe(001) magnetic tunnel junctions"

Recently, normal spinel type MgAl₂O₄ have attracted much attention, because the lattice constant of MgAl₂O₄ is about 8.09Å, leading to very small lattice mismatch less than 0.5% with bcc Fe. We investigated the spin-dependent transport properties of Fe/MgAl₂O₄/Fe(001) MTJs on the basis of first-principles calculations of the electronic structures and the ballistic conductance.

The calculated TMR ratio of a Fe/MgAl₂O₄/Fe(001) MTJ was about 160%, which was much smaller than that of a Fe/MgO/Fe(001) MTJ (1600%) for the same barrier thickness. However, there was an evanescent state with Δ_1 symmetry in the energy gap around the Fermi level of normal spinel MgAl₂O₄, indicating the possibility of a large TMR in Fe/MgAl₂O₄/Fe(001) MTJs. The small TMR ratio of the Fe/MgAl₂O₄/Fe(001) MTJ was due to new conductive channels in the minority spin states resulting from a band-folding effect in the two-dimensional Brillouin zone of the in-plane wave vector (k_{\parallel}) of the Fe electrode. Since the in-plane cell size of MgAl₂O₄ is twice that of the primitive in-plane cell size of bcc Fe, the bands in the boundary edges are folded, and minority-spin states coupled with the Δ_1 evanescent state in the MgAl₂O₄ barrier appear at k_{\parallel} = 0, which reduces the TMR ratio of the MTJs significantly.

2.1-A Mn-based Tetragonal and Inverse Heusler Alloy Films with Perpendicular Magnetic Anisotropy for Spin-Transfer-Torque application

(I) Magnetic and structural properties

We fabricated perpendicularly magnetized $Mn_{3-x}Ga$ (x=0-2) on Pt buffer, and investigated structure and magnetic properties of films with several composition x. Saturation magnetization Ms decreases with the composition close to x=0, and Ms was ~ 50 emu/cc. This trend is similar to that observed in bulk, however the peak intensity of (004) for $Mn_{3-x}Ga$ also decreases, so that structural disorders can be induced near the stoichiometric composition and deterioration of magnetic properties appeared in our view.

Furthermore, to get into insight the electronic structure of $Mn_{3-x}Ga$, we investigated magnetic moment and uniaxial (perpendicular) magneto-crystalline anisotropy Ku of epitaxial $Mn_{1-x}Ga$ thin films with much wider composition range from x=0-2. The epitaxial films with $L1_0$ structure ($x=\sim 1-2$) and with $D0_{22}$ structure ($x=\sim 2-3$) were nicely obtained with better qualities, which showed well-squared hysteresis loops when magnetic field is applied perpendicular to a film plane. Saturation magnetization and magnetic moment per unit cell decrease linearly with increasing Mn concentration. This can be explained by the model that Mn atom having the composition-independent magnetic moment occupies on different Mn site. The K_u is of the order of 10 Merg/cm³ in any compositions and did not decrease significantly against Mn composition x. The values for magnetic moment and K_u for these alloys roughly agree with the values predicted by first principle calculation done by Japanese theoretical group. These results demonstrated that Mn-Ga is a special material, namely the value of M_s can widely be tuned by Mn composition, and this is favorable for various kinds of application.

(II) Magnetization dynamics and Gilbert damping of Mn_{3-x}Ga films

We investigated the precessional dynamics of magnetization to evaluate Gilbert damping constant α for Mn_{3-x}Ga with L1₀ and D0₂₂ structures. Time-resolved magneto optical Kerr effect (TRMOKE) with Femtosecond pulse laser was employed to 100-300 GHz. Estimated Gilbert damping constant was evaluated to be at most 0.015 (0.007) for the 100 nm thick epitaxial Mn_{3-x}Ga_x films with D0₂₂ (L1₀) structures. These values are consistent with the theoretical fact, provided by Japanese theoretical group, that Gilbert damping for these alloys is not large. However, there still remains the issue whether the theoretical values agree with the experimental values quantitatively and why this Mn-Ga alloys show large K_u and small α simultaneously even though both quantities originate from spin-orbit interaction perturbing band structure for magnetic metals.

(III) TMR of MTJs with the Mn_{3-x}Ga electrodes

We first investigated TMR of MTJs with a perpendicularly magnetized $D0_{22}\text{-}Mn_{3-x}Ga$ (x=0.6) electrode. Staking structure was $D0_{22}\text{-}Mn_{3-x}Ga$ (30 nm) / Mg (0.4 nm) / MgO (2 nm)/ CoFe (2.5 nm). The maximum TMR ratio of 9.8% (22.1%) was observed at 300 K (10 K) with d_{Mg} = 0.4 nm. This value is quite smaller than the values estimated from the spin polarization of Mn₃Ga and CoFe electrodes. First principles calculations of band dispersion relations and tunneling conductance in a Mn₃Ga / MgO / Mn₃Ga layered structure were also performed by Japanese theoretical group, which revealed the existence of Δ_1 -bands in Mn₃Ga and relatively large TMR ratio over 600%. These are not consistent with the experimental results. To investigate if Mn atoms are oxidized at an interface between Mn-Ga and MgO, we investigated Mg layer thickness dependence on TMR in $D0_{22}$ -Mn_{2.4}Ga / Mg / MgO / CoFe MTJs. TMR ratio exhibited maximum value of 22% at d_{Mg} = 0.4 nm and - 14% at d_{Mg} = 1.4 nm at 10 K. The composition dependence of TMR in Mn-Ga / MgO / CoFe MTJs with Mn₅₄Ga₄₆, Mn₆₂Ga₃₈, and Mn₇₁Ga₂₉ electrodes was also investigated. An MTJ with a Mn₆₂Ga₃₈ electrode showed a maximum TMR ratio of 23% at 10 K and high annealing endurance up to 375 °C.

Although the bias voltage dependence of the TMR ratio was distinct among MTJs with different Mn-Ga compositions, TMR did not show significant composition dependences and seemed to be insensitive to Mn composition, even though electronic structure does change significantly with Mn composition. This may imply that TMR in these MTJs was determined by electronic structure at a

Mn-Ga / MgO interface. Therefore, we tried to modulate electronic structure at interface between Mn-Ga and MgO with inserting very thin iron or cobalt layers, as follows. In cases of iron insertion, we tested Mn₆₂Ga₃₈/Fe/MgO/CoFe structure. A maximum TMR ratio of 24% was observed in an MTJ with a Fe thickness of 1.1 nm at room temperature, which corresponded to a 57% TMR ratio in the case of a complete anti-parallel magnetization configuration. In case of Co insertion, we tested the fully perpendicular MTJs (p-MTJs) of Mn₆₂Ga₃₈/Co/MgO/CoFeB. The TMR ratio was improved significantly due to the Co insertion, reached 40% at room temperature (80% at 5 K) when the Co thickness was 1.5 nm.

2.2-A Half-metallic Heusler alloys combined with L10 ordered alloy films

(I) CPP-GMR with half-metallic Heusler compounds

In the project 2.2A, we have fabricated the CPP-GMR devices with CMS electrodes. The basic stacking structure is MgO-subs./Cr/Ag/CMS/Ag/CMS/Ag/Au. We have investigated annealing temperature dependence of MR ratio and successfully observed the largest MR ratio of 36% at RT and 68% at 110K in the sample annealed at 550°C. This MR ratio was the best MR ratio ever reported at that moment. We also investigated the mechanism of high MR ratio of CMS/Ag/CMS structure by obtaining a theoretical support from Prof. Shirai's group in this project. In the first principles calculation of ballistic conductance in (001)-oriented CMS/Ag/CMS and CMS/Cr/CMS structure, we found that Fermi surfaces of CMS and Ag have a similar shape with that of Cr, which results in a large conductance through the CMS/Ag interface. Therefore, we can expect a large conductance of majority-spin electron at the CMS/Ag, whereas a small conductance of minority-spin electron due to the half-metallicity of CMS, that seems to be a main origin of large MR ratio in (001)-oriented CMS/Ag/CMS CPP-GMR device. We also measured spin-torque induced rf-oscillation (STO) in the CMS/Ag/CMS CPP-GMR devices. STO is the phenomenon where the precession of magnetization around an effective magnetic is permanently excited by the balance between a damping torque and a spin-transfer torque. The rf-output power is generated from the changing of the device resistance through MR effect; thus the magnitude of rf-output power is determined from the MR ratio and the precession angle of magnetic moments around magnetic field. Owing to a large MR ratio of CMS/Ag/CMS CPP-GMR devices, we have successfully observed a large rf-output power of about 1 nW in spite of a small precession angle below 10 degree, which is one order of magnitude larger than that reported in usual CPP-GMR devices using a conventional 3d ferromagnetic material such as Fe and Co. In our more recent study, we have fabricated Co₂Fe_xMn_{1-x}Si(CFMS)-based CPP-GMR devices, and observed MR ratio of over 50% at RT. In these samples, we were able to observe the largest output power of 52 nW together with a large quality factor of over 1000.

(II) Anisotropic magnetoresistance effect in half-metallic Heusler compounds

Anisotropic magnetoresistance (AMR) effect is a conventional magnetoresistance effect in ferromagnetic materials, where an electric resistance changes with a relative angle f between magnetization and electric current directions. Recently, Kokado $et\ al.$ established a theoretical model to explain AMR effect universally on the basis of s-d scattering model with spin-orbit interaction. They reported that the sign of AMR ratio in half-metallic material should be always negative, i.e., a resistance in parallel state ($f=0^\circ$) is smaller than that in perpendicular state ($f=90^\circ$). In half-metallic materials, either up- or down-spin electron channel is missing at Fermi level, which result in a dominant s-d scattering from up- (down-) spin s-state to up- (down-) spin d-state; that is an origin of negative AMR ratio in half-metallic materials. If this theoretical prediction is correct, it is very useful to examine a half-metallicity of material since AMR effect can be easily measured by a general 4-terminal method without any micro-fabrications. Therefore, we have systematically investigated AMR effect in CFMS films with different compositions and annealing temperatures. As a result, when the Fe composition x varies in $\text{Co}_2\text{Fe}_x\text{Mn}_{1-x}\text{Si}$ epitaxial film, we observed the sign changes from negative to positive at x=0.8. According to the theoretical prediction by Kokado et al., this result suggested that a half-metallicity is perfectly destroyed over

x = 0.8. We also investigated the electronic structure of CFMS by first-principles calculation based on local density approximation. It was found from this calculation that the number of down-spin d-states gradually increases with x and finally a half-metallicity perfectly disappears in Co_2FeSi , which shows good agreement with the result of AMR measurement and theoretical model for AMR effect.

3.1-A Gilbert damping in half metal Heusler alloy films

From the theoretical and experimental researches on spin torque transfer switching, the magnitude of critical current density J_{C0} is considered to be proportional to damping constant (α) and saturation magnetization (M_S) and is inversely proportional to spin injection efficiency. Thus one needs materials showing low- α , low- M_S , and high-spin polarization. Half-metallic materials offer an ideal basis for a tailoring of the damping properties towards small α value because the energy gap for minority electrons closes the spin-flip channel as one of the important transfer mechanisms.

We fabricated epitaxially grown Co₂MnAl_xSi_{1-x} (CMAS) and Co₂Fe_xMn_{1-x}Si (CFMS) Heusler alloy films and systematically investigated their magnetic damping constant using a ferromagnetic resonance (FMR) technique. The relationship between the experimental results of the magnetic damping and the first principle DOS calculation has been clarified. Furthermore, we have also investigated thickness dependence of CFMS films. Finally, we have realized the very thin CFMS films with low magnetic damping. We provided the Heusler alloy films with low magnetic damping to the German groups and they have investigated the high-speed spin dynamics by pump-probe method and have also observed the spin-wave propagation. Detailed results are as follows.

Films with MgO(001)-sub./Cr(40)/CMAS or CFMS(30)/Ta(2) (in nm) structures were prepared using magnetron sputtering system. We controlled the film composition by co-sputtering from Co-Mn-Si (Co: 43.7%, Mn: 27.95%, Si: 28.35%), Co-Mn-Al (Co: 43.7%, Mn: 27.95%, Al: 28.35%), and Co-Fe-Si (Co: 47.5%, Fe: 24.2%, Si: 28.3%) alloyed targets. We used ICP spectroscopy to analyze the film compositions. The Co₂MnAl_xSi_{1-x} and the Co₂Fe_xMn_{1-x}Si films were annealed at 400°C and at 500°C respectively after deposition in order to increase the atomic site-ordering. The crystalline structure and magnetic properties were respectively characterized using x-ray diffraction (XRD) with Cu- K_a radiation and a superconducting quantum interference device (SQUID). The magnetic damping constant α and the magnetogyric ratio γ were measured by the FMR measurements using an X-band microwave source (f= 9.4 GHz) and a TE₀₁₁ cavity.

XRD results indicate that the fabricated CMAS films have a (001)-orientation and a B2-ordered structure, because a (002) peak originates in the superlattice reflections from the B2-ordered structure. The long-range order parameter of the B2 structure estimated from the peak intensities of (002) and (004) was 0.35-0.63. The epitaxitial growth was confirmed from the (220) peak observed in the pole–figure (ϕ -scan-profile) measurements for all CMAS films. The (111) peak from $L2_1$ -ordering was not detected from the pole–figure measurements except for in the Co₂MnSi film. The CFMS films also have a (001)-orientation. In addition, for all the CFMS films, the epitaxial growth and the $L2_1$ -ordering were confirmed from the (111) pole-figure measurements. The long-range order parameter of the $L2_1$ structure estimated from the (111) peak intensity was 0.2-0.9. However, the values of the estimated order parameters are not reliable, because the difference in atomic number is only 1 between the Co and Fe atoms.

The saturation magnetization values were about 20% lower than the values for the bulk samples, except for that for the Co₂MnAl film, indicating that the fabricated films included a certain amount of atomic site disorder. However, the saturation magnetization increases when the valence electron number systematically increases according to the Slater rule.

The Gilbert damping constant G ($G = \alpha \gamma M_s$) had the minimum value of 5.5×10^7 rad/s for the $Co_2Fe_{0.4}Mn_{0.6}Si$ film and increased rapidly for the $Co_2Mn_xFe_{1-x}Si$ with x > 0.6. The Gilbert damping constant is considered to be proportional to the square of the spin-orbit coupling parameter ξ and the total DOS at Fermi energy $D(E_F)$ as mentioned above. The electronic structure for the B2-ordered $Co_2MnAl_xSi_{1-x}$ and $L2_1$ -ordered $Co_2Fe_xMn_{1-x}Si$ alloys were calculated, although the

fabricated CMAS and CFMS films did not have complete $B2^-$ and $L2_1$ -ordered structures. The Gilbert damping constant measured by FMR technique seems to be roughly proportional to total calculated DOS at E_F . Small magnetic damping constant of $Co_2MnAl_xSi_{1-x}$ and $Co_2Fe_xMn_{1-x}Si$ (x < 0.6) may be attributed to their half-metallic property. In this region, the slight decrease of the magnetic damping constant with x is considered to be dominated by the DOS at E_F in majority spin states which is gradually decrease with increasing of the valence electrons number. In $Co_2Fe_xMn_{1-x}Si$ region, their half-metallic property is broken where E_F goes into the conduction band of minority spin states. It is possible to consider that the abrupt increasing of the magnetic damping constant of $Co_2Fe_xMn_{1-x}Si$ (x > 0.6) is explained by the contribution of the DOS in minority spin states. Such descriptions are consistent with our results of TMR effect in MTJs using $Co_2Fe_xMn_{1-x}Si$ electrode.

We have also investigated thickness dependence of magnetic damping constant for Co₂MnSi, Co₂Fe_{0.4}Mn_{0.6}Si (CFMS) and Co₂FeSi films. Magnetization of the CMS, CFMS and CFS films decreased significantly below 2 nm, however, magnetization saturated above 3 nm. This result indicates that the films above 3 nm had highly ordered structure. Magnetic damping constant of CMS and CFS drastically increased with decreasing the film thickness. On the other hand, magnetic damping constant of CFMS slightly increased by decrease of the film thickness. As a result, we have realized the 3 nm-thick-CFMS film with low magnetic damping constant of c.a. 0.01. The very thin CFMS film with low magnetic damping and high spin polarization would be very useful for the spintronic devices such as Spin-RAM, HDD head, high-frequency spin oscillator device and *etc*.

3.3-A Theoretical study of Gilbert damping in half metal Heusler alloy films

We have studied two subjects in this project. One is to calculate the Gilbert damping constants of the Heusler alloys by using the first principles approach based on the local density functional approximation (LDA). Another is to express both the charge and spin currents in the system of MTJ in the presence of bias voltage and spin dynamics. The main aim of this work is to present a microscopic description of these currents, in the same footing, including the GMR effects, spin transfer effects, charge and spin pumping effects, and the spin current driven by exchange interaction between magnetizations in both electrodes. In addition, we have succeeded to express the Gilbert damping constant in the system of non-uniform spin dynamics, which does not need the spin-orbit interaction.

To investigate the first item, that is the calculation of the Gilbert damping of the magnetic system, we started with the development of the calculation method of damping constants within the framework of the LDA including the spin-orbit interaction based on the Kambersky's theory combined with the linear response theory, and then tried to calculate the Gilbert damping constants α of Fe-Ni and Fe-Pt systems. The calculated value of α is given at $E-E_{\rm F}=0$ and is found to be about one half of the experimental result. The discrepancy may be reasonable, since we took into account only the electron scattering due to the random arrangement of atoms. In the next step, we evaluated the values of α of the Heusler alloys of Co₂MnAl, Co₂MnSi and Co₂FeSi with L2₁, B2 and A2 structures. For L2₁ and B2 structures, reflecting the intensity of the density of states (DOS) of each alloy, Co₂MnSi has the lowest value of α because it exhibits complete half metallicity, while in Co₂FeSi the electronic structure goes to metallic. In the A2 structure, they all become metallic system having peak in their DOS just at the $E_{\rm F}$, and the values of α are larger than those of other structures. Although this behavior is qualitatively consistent with the experimental results by Oogane's group, the values are about one tenth smaller than the experimental values. At this stage, the physical origin of this difference is not clear. Therefore, the quantitative investigations of the α of Heusler alloys in the bulk system together with the film structure will be the next subject of this item.

In the multilayered structures for the spintronics devices, it is considered that the spin damping can be attributed not only to the spin-orbit interaction mentioned above but also to the flows of angular momentum (spin currents) from the relevant magnetic layer to adjacent layers. Motivated by this situation, we have studied theoretically on the charge and spin transport in magnetic tunnel junctions (MTJs) on the basis of a tight-binding model. The spin and charge currents passing through the tunnel barrier are evaluated perturbatively with respect to the tunnel Hamiltonian. We assume that the ferromagnetic layer on the left-hand side of the MTJ is the free layer; that is, the direction of the field at time t in this layer, $M_L(t)$, rotates time-dependently. Thus, the direction of the field on the right-hand side (fixed layer), M_R , is time independent. As a result, we have found that the charge current have the form,

$$I_C(t) = C_1[\boldsymbol{M}_L(t) \times \dot{\boldsymbol{M}}_L(t)] \cdot \boldsymbol{M}_R + C_2 \dot{\boldsymbol{M}}_L(t) \cdot \boldsymbol{M}_R$$

where, C_1 and C_2 are constants. The first term represents the current drifted by the spin electric field. This term is time-independent when $M_L(t)$, steadily precess about the direction of M_R . The DC current induced by the spin dynamics also have been measured experimentally. While, the second term is certainly the AC current. For the spin current, we have

$$\boldsymbol{I}_{S}(t) = C_{3} \boldsymbol{M}_{L}(t) \times \boldsymbol{M}_{R} + C_{4} \dot{\boldsymbol{M}}_{L}(t) \times \boldsymbol{M}_{R} + C_{5} \boldsymbol{M}_{L}(t) \times \dot{\boldsymbol{M}}_{L}(t)$$
$$+ C_{6} [\dot{\boldsymbol{M}}_{L}(t) \cdot \boldsymbol{M}_{R}] \boldsymbol{M}_{L}(t) + C_{7} \dot{\boldsymbol{M}}_{L}(t) + C_{9} [\boldsymbol{M}_{L}(t) \cdot \boldsymbol{M}_{R}] \dot{\boldsymbol{M}}_{L}(t)$$

where the C_i 's are constants. Here we especially refer the third term which just describes the enhanced Gilbert damping. Comparison with $I_s(t)$ and the Landau Lifshitz Gilbert equation affords the following microscopic expression for the enhanced Gilbert damping constant

$$\Delta \alpha = \frac{\hbar}{2e^2 |\mathbf{S}_L|} \Gamma$$

where Γ is the tunnel conductance of the MTJ, and $|S_L|$ is the total spin polarization of the electrons in the free layer. From this expression, the size dependence of $\Delta\alpha$ can be described as follows:

$$\Delta \alpha \propto \frac{1}{\lambda}$$

where λ is thickness of the free layer, because $|S_L|$ is roughly proportional to the volume of the free layer, and Γ to the cross-sectional area of the barrier.

It was shown in the above study that the spin damping can take place in the magnetically inhomogeneous system even in the absence of the spin-orbit interaction. This leads us to expect that the non-uniform spin dynamics is also accompanied by the spin damping in the absence of the spin-orbit interaction. Then we have studied the Gilbert damping in bulk metallic ferromagnets containing magnetic and nonmagnetic impurities in the presence of non-uniform magnetization precession. In this model, a microscopic expression for the Gilbert damping tensor is obtained by using the linear response theory with respect to the interaction between magnetization and conduction electrons. We especially focus on a diagonal element of the tensor which is a conventional Gilbert damping constant, and evaluate it numerically as a function of the wave vector \mathbf{q} of magnetization precession. We found that the impurity scattering dominates Gilbert damping for $0 < |\mathbf{q}| < k_{\text{F}\uparrow} - k_{\text{F}\downarrow}$, while the Stoner excitation for $k_{\text{F}\uparrow} - k_{\text{F}\downarrow} < |\mathbf{q}| < k_{\text{F}\uparrow} + k_{\text{F}\downarrow}$ ($k_{\text{F}\,\text{S}}$ is the Fermi wave number for s spin electron).

4.1-B Novel devices based on Heusler films with GMR and MTJ nanocontacts

In the first period of this project, we fabricated STO devices composed of a continuous free layer without magnetic coupling with a magnetized fixed layer, and systematically measured the STO properties under a strong stray field from the fixed layer to discuss the anisotropic dispersion of the free layer.

The stacking structure of the multilayer was as follows: Si/SiO₂ substrate/Ta (5 nm)/Ru (50 nm)/Ta (5 nm)/Cu (5 nm)/Co₇₅Fe₂₅ (5 nm)/Cu (3 nm)/Co₇₅Fe₂₅ (15 nm)/Ru (7 nm)/Ta (2 nm) by dc

magnetron sputtering. In the fabrication process, electron-beam lithography and Ar ion milling were employed to form the nanocontact with a 100 × 120 nm² elliptical cross-section on the continuous free layer. CoFe (15 nm) was considered to be the "fixed" layer in terms of the spin transfer torque effect because its thickness was larger than that of the CoFe (5 nm) "free" layer. The free layer was only partially patterned so that a the spin current path would not spread into the Cu spacer. Ferromagnetic resonance (FMR) measurements were carried out using an X-band (9.7 GHz) microwave source and a TE102 model cavity. The sample was fixed on a quartz rod, and a goniometer was used to measure the out-of-plane angular ($\theta_{\rm H}$) dependences of the line width $(\Delta H_{\rm pp})$ and resonance field $(H_{\rm res})$ of the FMR spectra. The static magnetic properties were obtained from H_{res}. Microwave measurements between 1-14 GHz were carried out at room temperature using a spectrum analyzer. The current was varied between 0-20 mA in increments of 0.5 mA. Positive I was defined so that electrons would travel from the free layer to the fixed layer. The magnetic field was varied between 400 and 900 Oe in 100 Oe increments along the easy axis of the ellipse after a magnetic field of 3000 Oe was applied to make the magnetized state parallel. A preamplifier was used, but both the amplification and background noise have been subtracted from the data presented here.

Film 1 was composed of buffer/Co₇₅Fe₂₅ (5 nm)/Cu (3 nm), while film 2 was composed of buffer/Co₇₅Fe₂₅ (5 nm)/Cu (3 nm)/ferromagnetic layer (15 nm)/capping layer. Magnetic damping α was 0.009 and 0.015 for films 1 and 2, respectively. This indicates that α of film 2 increased since the flows of the spin angular momentum spread by the spin-pumping effect were scattered by the magnetization of the ferromagnetic layer. We considered the structure of the STO device used in this study. The STO device was composed of a continuous free layer with a nanocontact consisting of a nanopatterned spacer and a fixed layer. In this STO device, the free layer was free from the spin-pumping effect in the spin wave propagating region. This led to the small α, and hence, long propagation of the spin wave can be expected.

Top and bottom electrical contacts to the devices are patterned into coplanar waveguides to avoid RF losses. The RF transmission efficiency $\eta(\omega)$ was about 0.55 in any frequency. This reflection originates in the gap from 50 Ω of the device resistance according to our calculation. So, If 50 Ω devices were fabricated, STNO with very small RF transmission losses may be obtained. The resistance and GMR ratio of the STO device were 11.91 Ω and 0.76%, respectively. We discuss the magnetic state when H was swept from the negative to positive direction below. The magnetic state was parallel at -2000 Oe. As H was increased, the resistance increased, and the magnetic state became anti-parallel near the zero fields. This increase in resistance before the zero fields was due to the stray field ($H_{\rm stray}$) from the fixed layer. $H_{\rm stray}$ was not uniform and induced anisotropic dispersion of the free layer. The magnetic configuration of the free and fixed layer swas antiparallel near the zero-field. When H was increased, the magnetization of the fixed layer switched at approximately 300 Oe, and the anisotropy of the free layer was dispersed by $H_{\rm stray}$. The magnetic state became parallel at approximately 1100 Oe; therefore, $H_{\rm stray}$ was estimated to be approximately 1100 Oe. A strong $H_{\rm stray}$ can strongly couple the magnetized fixed layer and the free layer

A microwave signal appeared at oscillating frequency f = 7.0 GHz at 400 Oe. Higher harmonics waves were not observed. The frequency f decreased with increasing H until ~500 Oe, above which f increased monotonically. These tendencies were observed at the current we measured in this study (11–20 mA). f vs. H can be explained by theoretical predictions on the basis of the interplay between the external magnetic field and anisotropic field (H_a). In this experiment, H_a was small, while H_{stray} from the fixed layer was very large compared to H_{s} this suggests that the influence of H_{stray} resulted in the frequency dip at ~500 Oe. However, fitting using Kittel's formula disagreed with the experimental data. This means that the anisotropy dispersion shows simultaneous complexity with not only H_{stray} but also Oersted field and/or thermal fluctuations because of the large applied current. On the other hand, the line widths decreased with increasing H, which may be because the anisotropic dispersion of the free layer was suppressed by H. This means that the angle of stray field was distributed because of the elliptical shape of the fixed layer. These results show that H_{stray} caused the complicated oscillation mode in the free layer and broadened the

microwave spectra of this mode, and; therefore, it is important to control the anisotropic dispersion of the free layer.

The line width decreased with increasing current and reached the nallowest line width around 17 mA at which the maximum microwave power was shown; this was attributed to the suppression of thermal noise. The line width increased with the current and with a negative shift because of the increment in spin wave amplitude, which is consistent with theoretical predictions. In contrast, a positive shift was observed at the lower current region in the experiments, even though a small negative shift as a function of the current was predicted theoretically. The sign of the frequency shift is known to be negative in an in-plane magnetized film. For an in-plane magnetized anisotropic film, the sign of the frequency shift can be changed by controlling the magnetization angle of the free layer: when the direction of the magnetization of the free layer is the magnetic easy and hard axes, the sign can be positive and negative, respectively. In our experiments, the observed positive frequency shifts were caused by the combination of the stray field and the shift of the equilibrium orientation of the free layer induced by the spin transfer torque. For example, when an electron passes from the free layer to the fixed layer, the spin transfer torque can change the equilibrium orientation to be opposite to the magnetization of the fixed layer. This shift changes the amplitude of the effective magnetic field of the free layer: the contribution of the stray field increases, and that of the external magnetic field decreases. The stray field was relatively large compared to the external magnetic field. Therefore, the observed positive frequency shifts be related to the contribution of the stray field.

We can give the following conclusions. The damping constant of the free layer become small in the device structure without the fixed layer. And, the RF loss of the coplanar electrode was very small. In the CPP-GMR devices that were able to be evaluated electrically and optically, the microwave signals were observed. The RF frequency had little change for the current, while it showed a singular change for the magnetic field. Judged from these properties, it has been understood that a peculiar oscillation mode existed in the continuous free layer.

4.3-B Lateral spin transport in semiconductors

We have succeeded to demonstrate a new scheme of electrical magnetization reversal in (Ga,Mn)As through spin-orbit coupling effective field, the dependence of the universality classes of domain wall creep motion in (Ga,Mn)As on surface roughness, electrical spin injection from L1oFePt to GaAs through MgO barrier, and anisotropic carrier spin relaxation in (In,Ga)As quantum well. Such spin-related phenomena in ferromagnetic and nonmagnetic semiconductors are keys for realizing future spintronics devices, however, the studies based on Heusler compounds are still challenging due to the weak spin orbit interaction and difficulty for the epitaxial growth on semiconductors. Through the advanced researches on (Ga,Mn)As and metal/semiconductor hybrid structure, we contributed for promoting the research on spintronics devices based on Heusler compounds. Detailed results are explained below:

(I) New scheme of electrical magnetization reversal in (Ga,Mn)As through spin-orbit coupling effective field

We showed the M reversal by the application of the pulsed current j_P at 80 K. We initialize the M orientation along [110] by H, and then apply a positive j_P with width $w_P = 5$ µs. The j_P generates $H_{\rm eff}$ along [110] orientation, which reverses the M direction to [110] when H surpasses a threshold value. When the M reversal takes place, R_{yx} jump in the subsequent H sweep due to the clockwise M switching nearly along [010] to magnetization angle $\varphi \sim 270^{\circ}$ measured from [110] orientation across the hard axis. On the other hand, when M stays at the initial direction, no jump is observed in the counter-clockwise M rotation, because of the absence of the hard axis in the path. We found that the H dependence of R_{yx} after the application of $j_P = 1.7$ and 1.9 MA/cm². The jump observed in the trace for $j_P = 1.9$ MA/cm² clearly indicates the M reversal by j_P induced $H_{\rm eff}$. The absence of the jump for $j_P = 1.7$ MA/cm² indicates that no M reversal occurs at this j_P and the threshold current is the between the two j_P 's.

(II) Dependence of the universality classes of domain wall creep motion in (Ga,Mn)As on surface roughness

The dependence of DW velocity v on the magnitude of external magnetic field H is measured by magneto-optical Kerr effect (MOKE) microscope. In order to determine the universality classes of the DW creep, we fit the scaling formula $\ln(v/v_{\rm C}) = a - b(\mu_0 H)^{-\mu}$ to the experimental data by adopting scaling exponent μ as a fitting parameter, where a and b are expressed as the power of relative temperature (T-T_C) (T_C: the Curie temperature), v_C the velocity at the threshold drive, and μ ₀ the permeability in free space. The scaling exponent μ can be utilized to classify the universality class of the creep motion, and it is known that the creep with μ = 1 belongs to random-bond disorder, whereas that with μ = 0.25 to the random-field disorder. In the obtained m versus T/T_C, we can see clearly that value of μ is related to the buffer layer materials on which a (Ga,Mn)As is grown. DW creep motion in (Ga,Mn)As layer grown on (In,Al)As layer with flatter surface belongs to random-field disorder, whereas that in (In,Ga)As to random-bond disorder.

(III) Electrical spin injection from L1₀-FePt to GaAs through MgO barrier

We fabricated a spin injection device from a wafer consisting of 20 nm $L1_0$ -FePt / 2 nm MgO / 20 nm n^+ -GaAs (n^+ = 2×10¹⁹ cm⁻³) / 2 µm n-GaAs (n^+ = 3×10¹⁶ cm⁻³) / semi-insulating GaAs substrate. The MgO layer which forms a tunnel barrier was deposited at 400°C by electron beam deposition. The 20 nm $L1_0$ -Fe4₃Pt₅₇ layer was grown at 400°C by magnetron co-sputtering. Epitaxial growth of the $L1_0$ -FePt / MgO / GaAs structure was confirmed by Cu- $K\alpha$ X-ray diffraction. The spin injection device was patterned by standard photolithography and Ar ion milling where the 80 µm × 80 µm ferromagnetic (FM) contact B constitutes spin injector and detector while an Ohmic contact A and an FM contact C serve as reference electrodes. Distances between each contact are sufficiently longer than spin diffusion length in the n-GaAs channel. From the hysteresis loop, the ratio of remanent to saturation magnetization is determined to be 0.96. It enables us to inject the out-of-plane electron spins at zero magnetic field. We used three-terminal Hanle effect to probe spin accumulation at the interface of the channel beneath the FM contact B where constant spin injection current $I_{\rm inj}$ from contact B to C is applied while 3T-voltage from B to A is measured. Electron spin is injected into and extracted from n-GaAs channel when the current is negative and positive, respectively.

We achieved the electrical spin injection and detection from perpendicularly magnetized $L1_0$ -FePt / MgO into GaAs by using 3T-Hanle effect. It is found that the spin-RA product decreases with increasing temperature. These dependences can be explained by thermal and bias voltage variations of the TSP.

(IV) Anisotropic carrier spin relaxation in (In,Ga)As quantum well

The heterostructure which consists of 200 nm $In_{0.52}Al_{0.48}As$ for buffer layer / 6 nm $In_{0.52}Al_{0.48}As$ for carrier supply layer (Si doping with $N_d = 4.0 \times 10^{18}$ cm⁻³) / 15 nm $In_{0.52}Al_{0.48}As$ for spacer / 2.5 nm $In_{0.53}Ga_{0.47}As$ / 10 nm $In_{0.7}Ga_{0.3}As$ QW / 2.5 nm $In_{0.53}Ga_{0.47}As$ / 3 nm InP / 20 nm $In_{0.52}Al_{0.48}As$ / 1.5 nm AlAs / 5 nm $In_{0.52}Al_{0.48}As$ was processed into the gated narrow wires with 200 μ m long and 749 \pm 51 nm wide by electron beam lithography and reactive ion etching. For minimizing the universal conductance fluctuations, 95 narrow wires were arranged in parallel to the current paths and aligned along [110], [100] and [110] directions.

Gate voltage dependence of the magneto-conductance was measured at 1.7 K in the gate bias voltage range of -8.0 V < $V_{\rm g}$ < +5.5 V. Clear weak antilocalization (WAL) signals were observed for wires along the [1 $\bar{1}$ 0] and [100] directions in -8.0 V < $V_{\rm g}$ < +4.0 V. In the case of [110] direction, crossover from WAL to weak localization (WL) was observed by decreasing gate voltage. Since conductance minima are corresponding to the magnetic field in which the magnetic length becomes comparable to spin relaxation length, the strength of spin relaxation due to spin-orbit interaction (SOI) can be deduced from WAL signals. Conductance minima decrease by increasing gate voltages for all directions, indicating the weaker Rashba SOI due to decreasing of structure inversion

asymmetry inside quantum well. Furthermore, anisotropy of SOI obviously exists in the present samples. The polar plot of conductance minima, qualitatively indicating strength of spin splitting, for various gate voltages. By decreasing gate voltages from +5.5 V to -8.0 V, the spin splitting becomes more isotropic with the enhancement of SOI strength. This indicates that Rashba SOI which is spatially isotropic is getting much stronger and becomes dominant rather than Dresselhaus SOI by decreasing gate voltage. Spin splitting along [110] direction is the largest value of all directions due to constructive cooperation between Rashba and linear Dresselhaus SOI in contrast to destructive cooperation along [110] direction. Our experimental result clearly indicates that existence of both of Rashba and linear Dresselhaus SOIs and anisotropic spin relaxation depending on the crystal axis.

4.6-B Lateral spin transport in Heusler alloy systems

(I) Spin-Seebeck effect in Co₂MnSi epitaxial film

In the project of 4.6B, we investigated SSE in Co₂MnSi epitaxial film. The origin of SSE was initially explained by generation of spin-current due to thermally excited-nonequilibrium state of chemical potential for up and down spin electron. Therefore the first motivation to start this experiment is to investigate a SSE in half-metallic Co₂MnSi because a small/no SSE signal was expected in the case of ideal half-metallic materials. However, as a result of experiment, we observed clear SSE signal in an epitaxially grown Co₂MnSi films. The voltage of SSE in Co₂MnSi was almost same order of magnitude as that observed in Py. It was expected that the CMS epitaxial film has a higher spin-polarization than Py film at least by comparing MR ratios in CPP-GMR devices based on those materials. Therefore, our result implies that there is no strong relation between a spin-polarization of ferromagnetic metal and SSE. On the other hand, another important finding in this study was that a superposition of anomalous Nernst effect (ANE) in a measurement of the SSE. The signal of SSE was not symmetrically observed at high-temperature (HT) and low-temperature (LT) ends against zero voltage. We realized that the anomalous Nernst voltage superposed on the voltage from SSE is an origin of this asymmetry, since ANE voltage appears in same sign at HT and LT ends. The origin of ANE in this measurement is that an inevitable perpendicular temperature gradient in the CMS and Py films when we applied temperature gradient to the in-plane direction of the film. It was also found that the voltage of ANE is strongly enhanced at low temperature where a thermal conductivity of MgO substrate shows maximum. Therefore, we found in this study that a thermal conductivity matching between a substrate and a ferromagnetic film is important to study SSE without an artifact caused by ANE effect.

(II) Lateral spin-valve device with half-metallic Heusler compounds

To generate and detect a pure spin-current in non-magnetic metal/semiconductor is one of the important subjects in spintronics in order to realize new spintronics device such as spin-transistor. Half-metallic materials can be an ideal source and detector because of their large spin-polarization. In the project 4.6B, we also fabricated non-local lateral spin-valve (NLSV) devices using CFMS spin-injector and -detector and a Cu channel. In our device, we have clearly observed a large spin-accumulation signal ΔRs of over $4m\Omega$ at RT, which was one order of magnitude larger than that observed in NLSV with Co wire. The systematical analysis has not been completed yet, but there seems to be a further potential to enhance a spin-accumulation by improving a spin-resistance mismatching between CFMS and channel wires.

3 Project participants

3.1 Japanese Team 公開

Ando group (Organization of Team Leader)

Name	Organization, Division	Title	Specialty	Role in Project
Yasuo Ando	Tohoku Univ., Graduate school of engineering	Prof.	Spintronics	Team Leader and PI (4.1B), Design of nano-GMR/TMR device
Mikihiko Oogane	Tohoku Univ., Graduate school of engineering	Associate Prof.	Spintronic material	PI (3.4B), Spin injection into Si
Hiroshi Naganuma	Tohoku Univ., Graduate school of engineering	Assistant Prof.	Spintronic material	PI (1.1A)
Meng Khankhan	Tohoku Univ., Graduate school of engineering	Dr.	Spintronic material and device	Fablication of Heusler film and device

Takanashi group

Name	Organization, Division	Title	Specialty	Role in Project
Koki Takanashi	Tohoku Univ. Institute for Materials Research	Prof.	Magnetism, Spintronics	PI(2.2)
Yuya Sakuraba	Tohoku Univ. Institute for Materials Research	Assis. Prof.	Spintronics	Fabrication of the CPP GMR devices
Bosu Subrojati	Tohoku Univ. Institute for Materials Research	PD	Spintronics	Measurement of STO

Sakuma group

Name	Organization, Division	Title	Specialty	Role in Project
Akimasa Sakuma	Tohoku Univ., Graduate school of engineering	Prof.	Spintronics and materials	PI (3.3A), Gilbert damping

Tezuka group

Name	Organization, Division	Title	Specialty	Role in Project
Nobuki Tezuka	Tohoku Univ., Graduate school of engineering	Associate Prof.	Spintronic material and device	PI (1.1A)

Mizukami group

Name	Organization, Division	Title	Specialty	Role in Project
Shigemi Mizukami	Advanced Insitute for Materials Research	Associate Prof.	Spintronic Materials & Spin dynamics	PI(2.1A), Desgin of materials and physical analysis
Terunobu Miyazaki	Advanced Insitute for Materials Research	Prof.	Spintronic Materials& Magnetic tunnel junction	Desgin of structure
Takahide Kubota	Advanced Insitute for Materials Research	Research Associate	Spintronics Materials	Fablication of epitaxial thin films
Qinli Ma	Advanced Insitute for Materials Research	Research Associate	Magnetic tunnel junction	Fabrication of magnetic tunnel junction
Xiamin Zhang	Advanced Insitute for Materials Research	Research Associate	Magnetic tunnel junction	Charactrization of magnetic tunnel junction

Matsukura group

Name	Organization, Division	Title	Specialty	Role in Project
Fumihiro Matsukura	Tohoku Univ., WPI Advanced Institute for Materials Research	Prof.	Semiconductor spintronics	PI (4.3B), Lateral spin trasnport
Makoto Kohda	Tohoku Univ.Graduate school of engineering	Associate Prof.	Spintronics	Design of spin oribt interaction in semiconductors

3.2 German Team <mark>公開</mark>

P 1.2-A

Name	Organization, Division	Title	Specialty	Role in Project
Stanislav Chadov	MPI CPFS, AC	Dr.	Physics electronic structure, programming, computing	Leader
Binghai Yan	JGU, AC	Dr.	Surface chemistry electronic structure, computing	Leader
Jürgen Kübler	Emeritus	Prof. Dr.	Physics, electronic structure, programming, computing	Senior Scientist
NN	MPI CPFS, AC	Dipl. Phys	Ab-initio calculations	PhD student

P 1.3-A (Organization of Team Leader)

Name	Organization, Division	Title	Specialty	Role in Project
Fecher, Gerhard H.	MPI CPFS, AC	Dr.	Physics Magnetism, HAXPES, XMCD, Theory	Leader

Felser, Claudia	MPI CPFS, AC	Prof. Dr.	Inorganic Chemistry	Leader
Ouardi, Siham	MPI CPFS, AC	Dr.	Inorganic Chemistry Synthesis, HAXPES	Post Doc

P 1.5-B

Name	Organization, Division	Title	Specialty	Role in Project
Cinchetti, Mirko	TU-KL, PHYS	Dr. habil.	Physics Femtosecond magnetism, Interfaces with magnetic materials	Leader
Aeschlimann Martin	TU-KL, PHYS	Prof. Dr.	Physics Femtosecond magnetism, ultrafast phenomena at surfaces	Leader
Lösch, Marcel	TU-KL, PHYS	Dipl. Phys	Physics Spin-resolved photoemission, UHV systems	PhD student

P 2.4-A

Name	Organization, Division	Title	Specialty	Role in Project
Balke, Benjamin	JGU, AC	Dr.	Solid State Chemistry, Magnetism, HAXPES, Thermoelectrics	Leader
Cinchetti, Mirko	TU-KL, PHYS	Dr. habil.	Physics Femtosecond magnetism, Interfaces with magnetic materials	Leader
Aeschlimann, Martin	TU-KL, PHYS	Prof. Dr.	Physics Femtosecond magnetism, ultrafast phenomena at surfaces	Leader
Barkowski, Moritz	TU-KL, PHYS	Cand. Phys.	Physics TR-MOKE, all-optical switching	PhD student
Stinshoff, Rolf	JGU, AC	Dipl. Chem.	Inorganic Chemistry Synthesis	PhD student

P 4.7-B

Name	Organization, Division	Title	Specialty	Role in Project
Burkard Hillebrands	TU-KL, PHYS	Prof. Dr.	Physics Spin dynamics	Leader
Oleksandr Serha	TU-KL, PHYS	Dr.	Physics Magnon transport	Leader
Thomas Sebastian	TU-KL, PHYS	Dipl. Phys.	Magnon transport, SHE and STT phenomenon in Heusler films	PhD Student
Benjamin Jungfleisch	TU-KL, PHYS	Dipl. Phys.	Spin dynamics, Optical and electrical investigation of STNO	PhD Student

P 4.8-A

Name	Organization, Division	Title	Specialty	Role in Project
Ebke, Daniel	MPI CPFS, AC	Dr.	Physics Thin Films	Leader
Felser, Claudia	MPI CPFS, AC	Prof. Dr.	Inorganic Chemistry	Leader
Köhler, Albrecht	MPI CPFS, AC	Dipl. Phys.	Physics Thin Films	PhD Student

4 Project Deliverables of Japanese side

4.1 Publications 公開

The number of Japanese side publications in FY 2012

The number of coauthored publication in FY2012	5 publications
The number of Japanese publication in FY2012	30 publications

4.1.1 Coauthored Jointly by Japanese and German Teams

2010

(1) D. Steil, S. Alebrand, T. Roth, M. Krauß, T. Kubota, M. Oogane, Y. Ando, H. C. Schneider, M. Aeschlimann, and M. Cinchetti, "Band-Structure-Dependent Demagnetization in the Heusler Alloy Co₂Mn_{1-x}Fe_xSi," Phys. Rev. Lett. 105 (21), 217202 (2010).

2012

- (2) R. Fetzer, M. Lösch, Y. Ohdaira, H. Naganuma, M. Oogane, Y. Ando, T. Taira, T. Uemura, M. Yamamoto, M. Aeschlimann, and M.Cinchetti, "Revealing the spin and symmetry properties of the buried Co₂MnSi/MgO interface by low energy spin resolved photoemission," arXiv:1209.4368 [cond-mat.mtrl-sci] (2012).
- (3) R. Fetzer, J.-P. Wüstenberg, T. Taira, T. Uemura, M. Yamamoto, M. Aeschlimann, M. Cinchetti, "Structural, chemical and electronic properties of the Co₂MnSi(001)/MgO interface" arXiv:1209.5436, [cond-mat.mtrl-sci] (2012)
- (4) A. Gloskovskii, G. Stryganyuk, S. Ouardi, G. H. Fecher, C. Felser, J. Hamrle, J. Pistora, Subrojati Bosu, Kesami Saito, Yuya Sakuraba, and Koki Takanashi, "Structure determination of thin CoFe films by anomalous x-ray diffraction," J. Appl. Phys. 112, in press(2012).
- (5) J.-P. Wüstenberg, R. Fetzer, M. Aeschlimann, M. Cinchetti, J. Minár, J. Braun, H. Ebert, T. Ishikawa, T. Uemura, and M. Yamamoto, "Surface spin polarization of the nonstoichiometric Heusler alloy Co₂MnSi," Phys. Rev. B 85 (6), 064407 (2012).
- (6) T. Sebastian, Y. Ohdaira, T. Kubota, P. Pirro, T. Brächler, K. Vogt, A. A. Serga, Hiroshi Naganuma, M. Oogane, Y. Ando, and B. Hillebrands, "Low-damping spin-wave propagation in a micro-structured Co₂Mn₀.6Fe₀.4Si Heusler waveguide," Appl. Phys. Lett. 100, 112402 (2012).
- (7) A. Gloskovskii, G. Stryganyuk, G. H. Fecher, C. Felser, S. Thiess, H. Schulz-Ritter, W. Drube, G. Berner, M. Sing, R. Claessen, M. Yamamoto; "J. Electron Spectrosc. Relat. Phenom. 185 (2012) 47", J. Electron Spectrosc. Relat. Phenom. 185 (2012) 47.
- (8) S. Ouardi, G. H. Fecher, B. Balke, X. Kozina, C. Felser, T. Taira, and M. Yamamoto, "Hard X-ray photoelectron spectroscopy on buried, off-stoichiometric $Co_xMn_yGe_z$ (x : z = 2 : 0.38) Heusler thin films.", Appl. Phys. A submitted (2012).
- (9) Siham Ouardi, Takahide Kubota, Gerhard H. Fecher, Rolf Stinshoff, Shigemi Mizukami, Terunobu Miyazaki, Eiji Ikenaga, and Claudia Felser, "Stoichiometry dependent phase transition in Mn-Co-Ga-based thin films: From cubic inplane, soft magnetized to tetragonal perpendicular, hard magnetized," Appl. Phys. Lett. 101 242406 (2012).
- (10) S. Ouardi, C. E. Viol Barbosa, G. H. Fecher, M. Schwall, C. Felser, T. Kubota, S. Mizukami, T. Miyazaki, and E. Ikenaga "Investigation of interface properties of epitaxial Mn-Ga-thin films using hard x-ray photoelectron spectroscopy" Phys. Rev. B submitted (2012).
- (11) T. Sebastian and T. Bra¨cher, P. Pirro, A. A. Serga, and B. Hillebrands, T. Kubota, H. Naganuma, M. Oogane, Y. Ando, "Nonlinear Emission of Spin-Wave Caustics from an Edge Mode of a Microstructured Co2Mn0.6Fe0.4SiWaveguide" Phys. Rev. Lett., 110, 067201 (2013).

4.1.2 Authored by Japanese Team Only

2010

- (1) S. Bosu, Y. Sakuraba, K. Uchida, K. Saito, W. Kobayashi, E. Saitoh, and Koki Takanashi, "Thermal artifact on the spin Seebeck effect in metallic thin films deposited on MgO substrates," J. Appl. Phys. 111, 07B106 (2012).
- (2) M. Endo, F. Matsukura, and H. Ohno, "Current induced effective magnetic field and magnetization reversal in uniaxial anisotropy (Ga,Mn)As," Appl. Phys. Lett. 97, 222501 (2010).
- (3) A. Kanda, A. Suzuki, F. Matsukura, and H. Ohno, "Domain wall creep in (Ga,Mn)As," Appl. Phys. Lett. 97, 032504 (2010).

- (4) H. Nagunuma, T. Mayazaki, A. Ukachi, M. Oogane, S. Mizukami, and Y. Ando, "Structural characterization of epitaxial multiferroic BiFeO₃ films grown on SrTiO₃ (100) substrates by crystallizing amorphous Bi–Fe–O₂," J. Ceram. Soc. Jpn 118, 648 (2010).
- (5) M. Oogane, T. Kubota, Y. Kota, Shigemi Mizukami, Hiroshi Naganuma, A. Sakuma, and Y. Ando, "Gilbert magnetic damping constant of epitaxially grown Co-based Heusler alloy thin films," Appl. Phys. Lett. 96, 252501 (2010).
- (6) Y. Sakuraba, K. Izumi, T. Iwase, S. Bosu, K. Saito, K. Takanashi, Y. Miura, K. Futatsukawa, K. Abe, and M. Shirai, "Mechanism of large magnetoresistance in Co₂MnSi/Ag/Co₂MnSi devices with current perpendicular to the plane," Phys. Rev. B 82 (9), 094444 (2010).

2011

- (7) L. Bai, M. Kohda, and J. Nitta, "Observation of spin wave modes depending on a tunable periodic magnetic field," Appl. Phys. Lett. 98, 172508 (2011).
- (8) H. A. Begum, H. Naganuma, M. Oogane, and Y. Ando, "Fabrication of Multiferroic Co-Substituted BiFeO₃ Epitaxial Films on SrTiO₃ (100) Substrates by Radio Frequency Magnetron Sputtering," Materials 4, 1087 (2011).
- (9) T. Kubota, M. Araidai, S. Mizukami, X. Zhang, Q. Ma, H. Naganuma, M. Oogane, Y. Ando, M. Tsukada, and T. Miyazaki, "Composition dependence of magnetoresistance effect and its annealing endurance in tunnel junctions having Mn-Ga electrode with high perpendicular magnetic anisotropy," App. Phys. Lett. 99 (19), 192509 (2011).
- (10) T. Kubota, Y. Miura, D. Watanabe, S. Mizukami, F. Wu, H. Naganuma, X. Zhang, M. Oogane, M. Shirai, Y. Ando, and Terunobu Miyazaki, "Magnetoresistance Effect in Tunnel Junctions with Perpendicularly Magnetized D0₂₂-Mn₃₋₆Ga Electrode and MgO Barrier," Appl. Phys. Express 4, 043002 (2011).
- (11) T. Kubota, S. Mizukami, D. Watanabe, F. Wu, X. Zhang, H. Naganuma, M. Oogane, Y. Ando, and T. Miyazaki, "Effect of metallic Mg insertion on the magnetoresistance effect in MgO-based tunnel junctions using D0₂₂-Mn₃-δGa perpendicularly magnetized spin polarizer," J. Appl. Phys. 110, 013915 (2011).
 (12) Y. Miura, K. Abe, and M. Shirai, "Effects of interfacial noncollinear magnetic structures on spin-dependent
- (12) Y. Miura, K. Abe, and M. Shirai, "Effects of interfacial noncollinear magnetic structures on spin-dependent conductance in Co₂MnSi/MgO/Co₂MnSi magnetic tunnel junctions: A first-principles study," Phys. Rev. B 83 (21), 214411 (2011).
- (13) Ý. Miura, K. Futatsukawa, S. Nakajima, K. Abe, and M. Shirai, "First-principles study of ballistic transport properties in Co₂MnSi/X/Co₂MnSi(001) (X= Ag, Au, Al, V, Cr) trilayers," Phys. Rev. B 84 (13), 134432 (2011).
- (14) S. Mizukami, F. Wu, A. Sakuma, J. Walowski, D. Watanabe, T. Kubota, X. Zhang, H. Naganuma, M. Oogane, Y. Ando, and T. Miyazaki, "Long-Lived Ultrafast Spin Precession in Manganese Alloys Films with a Large Perpendicular Magnetic Anisotropy," Phys. Rev. Lett. 106 (11), 117201 (2011).
- (15) T. Saito, N. Tezuka, and S. Sugimoto, "Electrical Transport Properties and Spin Injection in Co₂FeAl_{0.5}Si_{0.5}/GaAs Junctions," IEEE T. Magn. 47, 2447 (2011).
- (16) Y. Sakuraba, K. Izumi, S. Bosu, K. Saito, and K. Takanashi, "Temperature dependence of spin-dependent transport properties of Co₂MnSi-based current-perpendicular-to-plane magnetoresistive devices," J. Phys. D: Appl. Phys. 44 (6), 064009 (2011).
- (17) R. Okura, Y. Sakuraba, T. Seki, K. Izumi, M. Mizuguchi, and K. Takanashi, "High-power rf oscillation induced in half-metallic Co₂MnSi layer by spin-transfer torque," Appl. Phys. Lett. 99, 052510 (2011).
- (18) A. Sasaki, N. Tezuka, L Jiang, and S. Sugimoto, "Magnetoresistance effect of tunnel junctions using Co₂(Ti, Mn)Z (Z=Al, Si) Heusler alloys," J. Appl. Phys. 109, 07C736 (2011).
- (19) F. Wu, S. Mizukami, D. Watanabe, H. Naganuma, M. Oogane, Y. Ando, and T. Miyazaki, "Influence of composition on structure and magnetic properties of epitaxial Mn-Ga films," J. Phys.: Conf. Ser. 266 (1), 012112 (2011).

2012

- (20) T. Kubota, Q. Ma, S. Mizukami, X. Zhang, Y. Miura, H. Naganuma, M. Oogane, Y. Ando, and T. Miyazaki, "Dependence of Tunnel Magnetoresistance Effect on Fe Thickness of Perpendicularly Magnetized L1₀-Mn₆₂Ga₃₆/Fe/MgO/CoFe Junctions," Appl. Phys. Express 5, 043002 (2012).
- (21) Y. Kunihashi, M. Kohda, and J. Nitta, "Semiclassical approach for spin dephasing in a quasi-one-dimensional channel," Phys. Rev. B 85 (3), 035321 (2012).
- (22) Q. Ma, T. Kubota, S. Mizukami, X. Zhang, H. Naganuma, M. Oogane, Y. Ando, and T. Miyazaki, "Magnetoresistance effect in L1₀-MnGa/MgO/CoFeB perpendicular magnetic tunnel junctions with Co interlayer," Appl. Phys. Lett. 101 (2012).
- (23) H. Naganuma, K. Sone, I.-T. Bae, T. Miyazaki, J. Miura, T. Nakajima, and O. Soichiro, "Structural Analyses of Coand Mn-Substituted BiFeO₃ Polycrystalline Films," Jpn. J. Appl. Phys. 51, 061501 (2012).
- (24) S. Naghavi, S. Chadov, C. Felser, G. H. Fecher, J. Kübler, K. Doll, and M. J.sen, "Pressure induced insulator/half-metal/metal transition in a strongly correlated p-electron system," Phys. Rev. B 85, 205125 (2012).
- (25) S. Nonaka, Y. Kunihashi, M. Kohda, and J. Nitta, "Anisotropic Weak Anti-Localization under In-Plane Magnetic Field and Control of Dimensionality via Spin Precession Length" Jpn. J. Appl. Phys. 51, 04DM01 (2012).
- (26) R. Ohsugi, M. Kohda, T. Seki, A. Ohtsu, M. Mizuguchi, K. Takanashi, and J. Nitta, "MgO Layer Thickness Dependence of Structure and Magnetic Properties of L1₀-FePt/MgO/GaAs Structures," Jpn. J. Appl. Phys. 51, 02BM05 (2012).
- (27) T. Saito, N. Tezuka, and S. Sugimoto, "Temperature and Bias Voltage Dependencies of Spin Injection Signals for Co₂FeAl_{0.5}Si_{0.5}/n-GaAs Schottky Tunnel Junction," Mater. T JIM 53, 641 (2012).

- (28) T. Saito, N. Tezuka, and S. Sugimoto, "Structural and Magnetic Properties of Co₂FeAl_{0.5}Si_{0.5} Full-Heusler Alloy Thin Films on GaAs Substrates," Mater. T JIM 53, 370 (2012).
- (29) N. Tezuka, "New materials research for high spin polarized current" J. Mag. Magn. Mater. 324 (21), 3588 (2012).
- (30) N. Tezuka, F. Mitsuhashi, and S. Sugimoto, "Tunnel magnetoresistance effect in magnetic tunnel junctions with
- epitaxial Co₂FeAl_{0.5}Si_{0.5}Heusler electrodes on MgO (110) single substrates" J. Appl. Phys. 111, 07C718 (2012). (31) S. Tsunegi, Y. Sakuraba, K. Amemiya, M. Sakamaki, E. Ozawa, A. Sakuma, K. Takanashi, and Y. Ando, "Observation of magnetic moments at the interface region in magnetic tunnel junctions using depth-resolved x-ray magnetic circular dichroism," Phys. Rev. B 85 (18), 180408 (2012).
- (32) F. J. Yang, Y. Sakuraba, S. Kokado, Y. Kota, A. Sakuma, and K. Takanashi, "Anisotropic magnetoresistance in Co₂(Fe,Mn)Si Heusler epitaxial films: A fingerprint of half-metallicity," Phys. Rev. B 86 (2), 020409 (2012).
- (33) S. Mizukami, T. Kubota, F. Wu, X. Zhang, T. Miyazaki, H. Naganuma, M. Oogane, A. Sakuma, and Y. Ando, "Composition dependence of magnetic properties in perpendicularly magnetized epitaxial thin films of Mn-Ga alloys," Phys. Rev. B 85 (1), 014416 (2012).
- (34) H. Liu, Y. Honda, T. Taira, K.-i. Matsuda, M. Arita, T. Uemura, and M. Yamamoto; "Giant tunneling magnetoresistance in epitaxial Co₂MnSi/MgO/Co₂MnSi magnetic tunnel junctions by half-metallicity of Co₂MnSi and coherent tunneling", Appl. Phys. Lett. 101, 132418 (2012).
- (35) T. Saito, N. Tezuka, M. Matsuura and S. Sugimoto, "Non-local and Local Spin Signals in a Lateral Spin Transport Device with Schottky Tunnel Junctions," IEEE Trans. Magn., accepted.
 (36) T. Saito, N. Tezuka, M. Matsuura and S. Sugimoto: Three-Terminal Hanle Signals in Schottky Tunnel Junctions
- with Co2FeAl0.5Si0.5 Full-Heusler Alloy Electrodes Deposited at Various Temperatures . Jpn. J. Appl. Phys,. accepted (37) Hiromi Shima, Ken Nishida, Takashi Yamamoto, Toshiyasu Tadokoro, Koichi Tsutsumi, Michio Suzuki, and Hiroshi Naganuma "Large refractive index in BiFeO3-BiCoO3 epitaxial films" Journal of Applied Physics, 113, 17A914-1-3 (2013). (38) Keita Sone, Sho Sekiguchi, Hiroshi Naganuma, Takamichi Miyazaki, Takashi Nakajima, and Soichiro Okamura 'Magnetic properties of CoFe2O4 nanoparticles distributed in multiferroic BiFeO3 matrix' Journal of Applied Physcis, 111,
- (39) Y. Miura, S. Muramoto, K. Abe and M. Shirai, "First-principles study of tunneling magnetoresistance in Fe/MgAl2O4/Fe(001) magnetic tunnel junctions", Physical Review B, 86, 024426/1-6, (2012).
- (40) Y. Sakuraba, M. Ueda, Y. Miura, K. Sato, S. Bosu, K. Saito, M. Shirai, T. J. Konno, and K. Takanashi, "Extensive study of giant magnetoresistance properties in half-metallic Co2(Fe,Mn)Si-based devices", Applied Physics Letters, 101, 252408/1-3, (2012).
- (41) Q. L. Ma, T. Kubota, S. Mizukami, X. M. Zhang, M. Oogane, H. Naganuma, Y. Ando, and T. Miyazaki, "Annealing Temperature and Co Layer Thickness Dependence of Magnetoresistance Effect for L10-MnGa/Co/MgO/CoFeB Perpendicular Magnetic Tunnel Junctions," IEEE Trans. Mag. 48, 2 (2012).
- (42) Yuya Sakuraba, Kota Hasegawa, Masaki Mizuguchi, Takahide Kubota, Shigemi Mizukami, Terunobu Miyazaki, and Koki Takanashi, "Anomalous Nernst Effect in L10-FePt/MnGa Thermopiles for New Thermoelectric Applications," Applied Physics Express 6, 033003 (2013).
- (43) T. Kubota, Q. L. Ma, S. Mizukami, X. M. Zhang, H. Naganuma, M. Oogane, Y. Ando, and T. Miyazaki, "Magnetic tunnel junctions of perpendicularly magnetized L10 MnGa/Fe/MgO/CoFe structures: Fe-layer-thickness dependences of magnetoresistance effect and tunneling conductance spectra," J. Phys. D 46 155001 (2013).
- (44) S. Bosu, Y. Sakuraba, K. Uchida, K. Saito, W. Kobayashi, E. Saitoh, K. Takanashi, "Thermal artifact on the spin Seebeck effect in metallic thin films deposited on MgO substrates" J. Appl. Phys. 111, 07B106 (2012).
- (45) D. Miura and A. Sakuma, "Microscopic Theory of Magnon-Drag Thermoelectric Transport in Ferromagnetic Metals", J. Phys. Soc. Jpn., 81 (2012) 054709.
- (46) N. Umetsu, D. Miura and A. Sakuma, "Microscopic theory for Gilbert damping in materials with inhomogeneous spin dynamics", J. Appl. Phys., 111 (2012) 07D117.
- (47) N. Umetsu, D. Miura and A. Sakuma, "Theoretical Study on Gilbert Damping of Nonuniform Magnetization Precession in Ferromagnetic Metals", J. Phys. Soc. Jpn., 81 (2012) 114716.
- (48) A. Sakuma, "First-Principles Study on the Gilbert Damping Constants of Transition Metal Alloys, Fe-Ni and Fe-Pt Systems", J. Phys. Soc. Jpn., 81 (2012) 084701.
- (49) Yuki Kawada, Hiroshi Naganuma, Mikihiko Oogane, and Yasuo Ando, "Influence of stray field from a nano-patterned fixed layer to the continuous free layer on spin torque oscillation," J. Mag. Mag. Mat., under review.
- (50) A. S. Demiray, T. Miyawaki, Y. Watanabe, M. Kohda, K. Saito, S. Mitani, K. Takanashi, and J. Nitta, "Relative vortex state control in a Co/Cu/Co pseudo-spin-valve ring", Japanese Journal of Applied Physics,. 51, (2012) 04DM04
- (51) A. S. Demiray, M. Kohda, T. Miyawaki, Y. Watanabe, K. Saito, S. Mitani, K. Takanashi, and J. Nitta, "Electrical determination of relative chirality direction in a Co/Cu/Co ferromagnetic ring", Appl. Phys. Lett. 101, 062409-1 - 062409-5
- (52) M. Kohda, S. limori, R. Ohsugi, H. Naganuma, T. Miyazaki, Y. Ando, and J. Nitta, "Structural and magnetic properties of L1₀-FePd/MgO films on GaAs and InP lattice mismatched substrates", Appl. Phys. Lett. 102, 102411 (2013).